SIZE-SELECTIVE MONITORING TECHNIQUES FOR PARTICULATE MATTER IN CALIFORNIA AIR

Final Report, Interagency Agreement (ARB No. A5-00487)

Prepared by

Walter John, Georg P. Reischl and Jerome J. Wesolowski

February 1978

Air and Industrial Hygiene Laboratory
Laboratory Services Branch
California Department of Health
2151 Berkeley Way
Berkeley, California 94704
(415) 843-7900, ext. 595

The statements and conclusions in this report are those of the Contractor and not necessarily those of the State Air Resources Board. The mention of commercial products, their source or their use in connection with material reported herein is not to be construed as either an actual or implied endorsement of such products.

ABSTRACT

After a review of the criteria for a suitable size-selective monitoring instrument, the dichotomous virtual impactor and the cyclone were selected for evaluation. A cyclone was designed with a 50% cutoff of 3.5 μm at 15 ℓ/min. The cyclone and the Sierra Model 243 dichotomous virtual impactor were tested extensively with monodisperse aerosol including both solid and liquid particles. Detailed measurements were made of particle deposition in the samplers as a function of particle size and air flow rate. Wall losses, reentrainment and uniformity of filter deposits were determined. The results of the tests show that both samplers are satisfactory for monitoring purposes.

A preliminary investigation was made of the stacked filter unit. Measurements of the filtration efficiency of the 8 μm pore size Nuclepore filter indicate that particle bounce is an important problem and that the particles are sized geometrically. Additional work is necessary to establish the characteristics of the stacked filter unit.

A manifold was designed for particulate sampling in ambient air. The inlet has a 50% cutoff of 20 μm. A new impaction surface, oil-soaked sintered metal, eliminates particle bounce, even with heavy loading. The manifold is equipped with an eight sector wind run acquisition system.

EXECUTIVE SUMMARY

Because the adverse effects of particulate matter depend on particle size, it is necessary to develop a size-selective monitoring technique for particulate matter in California air. Solution of this problem requires the analysis of the goals of the monitoring, selection of possible techniques to satisfy these goals, and a critical evaluation of these techniques including experimental testing.

After a review of the criteria for a suitable size-selective monitoring instrument, the dichotomous virtual impactor and the cyclone were selected for evaluation. A cyclone was designed for sampling of ambient air. The cyclone and the Sierra Model 243 dichotomous virtual impactor were tested extensively with well-characterized laboratory aerosol including both solid and liquid particles. Detailed measurements were made of particle deposition in the samplers as a function of particle size and air flow rate. Wall losses, reentrainment and uniformity of filter deposits were determined. The results of the tests show that both samplers have satisfactory sampling characteristics and acceptable particle losses. The comparative advantages of the two samplers are discussed.

During the project period, a new size-selective sampler, the Stacked Filter Unit (SFU) was developed at U.C., Davis. While not satisfying the criteria for a general purpose size-selective monitoring device, the SFU represents a low cost special purpose particulate sampler which may be useful for studies requiring an array of samplers. Therefore, the present study included some laboratory tests of the SFU. The preliminary investigation has revealed that particle bounce is an important problem and that particles are sized primarily by geometric rather than aerodynamic diameter. Additional work is needed to further explore these effects as well as to answer

a number of remaining questions including the variation of the filtration characteristics with particle material, particle size, air flow rate, filter pore size and particle loading.

In anticipation of the need for parallel testing of several size-selective particulate samplers in ambient air, a manifold was designed and constructed. The inlet has a cutoff at 20 μm particle diameter provided by a novel impaction surface, oil-soaked sintered metal, which eliminates particle bounce-off even with heavy loading. The manifold is also equipped with an eight sector wind run acquisition system.

CONTENTS

I. INTRODUCTION

Because the adverse effects of particulate matter depend on particle size, it is necessary to develop a size-selective monitoring technique for particulate matter. Solution of this problem requires the analysis of the goals of the monitoring, selection of possible techniques to satisfy these goals, and a critical evaluation of these techniques including experimental testing.

There is increasing concern that particulate matter in the ambient air of California may be inadequately monitored owing to reliance on the high-volume sampler. The hi-vol does not yield data on particle size; such data are required for the proper assessment of the adverse effects of particulate pollutants. The particle size distribution determines the amount of toxic material deposited in various sites within the human respiratory system[1] and the extent of visibility impairment.[2] Particle size is an important parameter linked to the particle source, whether it be natural or anthropogenic.[3,4] Thus, if the data for particulate-matter monitoring is to be used as a basis for control strategy, it should be based on size-selective sampling.

Given the need for size-selective sampling, the problem is to identify a suitable monitoring technique. There are a number of size-selective samplers which might be considered. However, the number can be narrowed to two, namely, the cyclone and the dichotomous virtual impactor, by a critical analysis based on the objectives of size-selective monitoring. This is presented in the next section.

None of the size-selective samplers currently available has been sufficiently tested to permit their deployment in a monitoring network with assurance of satisfactory performance. Laboratory testing under con-

trolled conditions should precede the use of samplers in the field to ensure the collection of valid data. Using monodisperse laboratory aerosols, the collection efficiency can be measured as a function of particle size. Tests are necessary with sticky and bouncy particles. Effects which should be evaluated include wall losses, particle bounce-off, reentrainment, uniformity of filter deposits and the effect of loading and air flow rate on sampling efficiency.

The two sampling systems selected for evaluation, the cyclone[5] and the dichotomous virtual impactor[6], were submitted to extensive laboratory testing. The experimental results are presented in this report as well as a discussion of the suitability of the samplers for use in monitoring, based on the laboratory tests. The present project also included the development of a sampling manifold which can be used for parallel testing of particulate matter samplers in ambient air.

During the project period, a new size-selective sampler, the Stacked Filter Unit (SFU) was developed at U.C., Davis.[7] This attractively simple sampler deposits a fine and coarse particle fraction on two Nuclepore filters suitable for automated elemental analysis by X-ray fluorescence. While not satisfying the criteria for a general purpose size-selective monitoring device, the SFU represents a low cost special purpose particulate sampler which may be useful for studies requiring an array of samplers. Therefore, the present study included some preliminary laboratory tests of the SFU.

II. SELECTION OF TECHNIQUES TO BE EVALUATED

We present here the rationale for the choice of two systems to be tested -- the dichotomous virtual impactor and a cyclone-total filter combination. These two systems have in common the aerodynamic separation of the particles into two size ranges deposited on filters. The criteria for selection of these two techniques for evaluation follow:

A. Separation by aerodynamic diameter

One of the parameters controlling the deposition of material in the respiratory system is the particle aerodynamic diameter, which is dependent upon the geometrical size, density and shape. The division of the deposited material among the nasal, tracheobronchial and pulmonary compartments depends on the aerodynamic diameter.[1] Therefore, the particle sampler must utilize aerodynamic separation of the particle sizes. Other, indirect sizing techniques based on optical or electrical properties are ruled out since the complications of ambient aerosol preclude relating the data to aerodynamic diameter.

B. Sampling for chemical analysis

The toxicity of respired material depends on the chemical species. This requires that a sample of the material be acquired for chemical analysis in the laboratory. The complexity of the particle chemistry excludes the possibility of real-time analysis for most compounds of interest. Chemical analysis is necessary to determine compliance with air quality standards, for identification of the sources of the aerosol and for correlation with visibility.

C. Mass determination

Filter samples enable direct mass determination to be made gravimetrically. Particle counting techniques are ruled out since the mass cannot be calculated reliably for ambient aerosol. Conventional cascade impactors require a sticky substrate on the collection surfaces. This makes gravimetric mass determination difficult under field conditions.

D. Correlation with visibility

In two recent studies, the refined particle fraction has been successfully correlated with visibility. One study utilized a two-stage impactor with beta gauges for mass measurement.[8] The second study was based on X-ray fluorescence analysis of samples from a three-stage impactor.[9] Visibility data were well fitted by only a few terms, each term representing the concentration of an element in a certain particle size range. It is noteworthy that none of the terms involved the coarse particle fraction. The ACHEX study[10] produced an equation for visibility based on chemical analysis without mass refinement. However, this was based mainly on data from areas where the visibility impairment was dominated by photochemical aerosol. An earlier study in California[11] found mass concentration to be a poor measure of visibility; moreover, the use of refined mass provided no improvement. On the basis of these studies, it appears that refined mass coupled with chemical analysis is required to yield correlations to visibility under various conditions.

E. Practical considerations

The techniques chosen must be suitable for routine monitoring under field conditions. The number of samples generated must be kept to the minimum consistent with acquisition of the desired data. This limits the number of cuts which can be made in the size distribution. The two systems chosen for study separate the particles into just two size ranges. That this may be sufficient is suggested by two considerations. First, respirable dust has been defined as that

portion of the inhaled dust which penetrates to the non-ciliated portions of the respiratory tract.[1,12] The American Conference of Governmental Industrial Hygienists (ACGIH) has designated 3.5 μm (equivalent unit density spheres) as the aerodynamic diameter where 50% of the dust is respirable.[12] The ACGIH also specified the percent respirable as a function of aerodynamic diameter. The specified curve is closely approximated by the penetration curve of cyclones which have been developed for sampling of respirable dust.

Secondly, studies[3,4,10] of the particle size distribution of ambient aerosols at a number of locations including Los Angeles have revealed a characteristic trimodal distribution consisting of a nuclei mode (< 0.1 μm), an accumulation mode (0.1-1 μm) and a coarse particle mode (> ca 2 μm). The nuclei mode is attributed to fresh aerosol from combustion sources including automobiles which rapidly coagulates into the accumulation mode. In addition to these primary aerosol constituents, the accumulation mode contains practically all of the aerosol mass from chemical reactions in the atmosphere while the coarse particles represent largely windblown or mechanically generated dust particles.

For the present discussion, the important points are the relatively fixed size ranges for the different modes and the location of the minimum between the accumulation and coarse particle modes at approximately 2 μm. Since this value is near the 3.5 μm, 50% respirable diameter, it is possible that a single size cut may serve to distinguish the respirable fraction as well as the nuclei and accumulation modes from the coarse particle mode. It should be emphasized that the sampling into two size fractions must be accompanied by chemical analysis of the deposits in order to adequately characterize the ambient aerosol.

Finally, the selection of sampling systems is made here for monitoring purposes, not for research into the properties of ambient aerosol. It is anticipated that additional data on ambient particles may be

required for special problems. This requirement should be met by temporary deployment of specialized samplers.

F. Disadvantages of conventional cascade impactors

We summarize here the shortcomings of conventional cascade impactors:

1. Particle bounceoff from the stages.[13,14]
2. Sticky substrates make accurate mass determination difficult.
3. The effective substrate changes as particles build up on the stages.
4. Reentrainment of particles which are blown off the stages by the air jets.
5. Wall losses within the impactors.
6. Highly non-uniform deposits.

Some cascade impactors use a filter substrate. These include the cascade impactor which operates on a conventional hi-vol sampler. However, the filter substrate has been found to spoil the impactor particle size cutoff characteristics.[14] The filter is found to trap some of the small particles which normally pass through a given impactor stage, presumably because the air jet penetrates the surface of the filter to some extent. A Canadian study[15] involving extensive field work recommended against the use of certain impactors tested for monitoring. These impactors included the Andersen, BGI-30 and Sierra Hi-Volume Cascade Impactors. Significant differences were found between total particulate as measured by the cascade impactors and the conventional hi-vol.

G. Summary of the specific advantages of the cyclone and the dichotomous virtual impactor systems

1. Both systems separate the particle size fractions aerodynamically.
2. Both systems deposit the particulate matter on filters.
3. The filter deposits are relatively uniform over the area, facilitating accurate chemical analysis.
4. Both systems segregate the particles into just two size ranges.

5. The cyclone's particle size cutoff characteristics can be made to closely parallel the accepted respirable dust curve. The cyclone is the instrument widely used for health effects studies.
6. The cyclone can be scaled up to high flow rates.
7. The virtual sampler deposits the coarse fraction on a separate filter for analysis.
8. Both systems are free of the problems which plague cascade impactors, namely, particle bounceoff and reentrainment.
9. Both systems can accommodate requirements for monitoring for new chemical species.

III. DEVELOPMENT AND TESTING OF A CYCLONE SAMPLER

A. Cyclone sampler design

Cyclones have been used for decades for air cleaning[16,17] and for evaluation of respiratory hazards in industrial hygiene applications.[5,12] They have seen limited use for atmospheric sampling. Since no suitable commerical cyclone was available, one was developed for the present application.

The following criteria were adopted for the cyclone sampler design:

1. The cyclone is to have the "standard" geometry, namely, a vertical cone with a cup on the bottom and the outlet at the top. There is more experience with this geometry, and it may minimize loading and reentrainment, although there is little comparative data on other geometries.
2. The particle size cutoff should be sharp and the 50% particle size cut point should be 3.5 μm aerodynamic diameter.
3. The after-filter should be 47 mm in diameter. This is near the minimum diameter which will give sufficient sample for chemical analysis. It also allows the use of membrane filters such as Fluoropore☆ which are suitable for x-ray and wet chemical analysis and which also have low artifactual sulfate and nitrate formation.
4. The cyclone will be used for 24-hour sampling. This requirement combined with the choice of a 47 mm membrane filter implies a flow rate of approximately 15 ℓ/min. (0.6 CFM) in view of the anticipated filter loading with ambient air.

☆Millipore Corporation, Bedford, MA.

5. The cyclone geometry should be precisely determined. This requires machining from solid metal rather than fabrication from sheet metal.
6. The inner surface of the cone should be designed to maintain its characteristics under exposure to ambient air. The condition of the surface could affect the deposition of particles. Therefore, it was made of aluminum which was polished and then anodized.
7. The instrument should be readily disassembled for cleaning and the pressure seals should be dependable. For convenience, the entire cyclone assembly was equipped with a quick-disconnect at the junction to the intake pipe. The after-filter holder was also equipped with a quick-disconnect to facilitate exchange with a preloaded filter holder. All breakable connections are sealed by O-rings including the seal to the filter. The latter is an important consideration because it is difficult to seal Fluoropore filters.

No commercial cyclone satisfied the above criteria. However, the Southern Research Institute[18] has developed a cyclone for stack sampling based on the T-2A cyclone designed by Chang.[19] Our sampler is similar to the SRI cyclone, all of the critical cyclone dimensions being the same. An assembly drawing is shown in Figure 1. The important dimensions are listed in Table 1. The after-filter holder is a 47 mm Gelman☆ filter holder, No. 1235. Most of the tests were made on the sampler as shown in Figure 1. As explained below, in order to improve the uniformity of the deposit on the after-filter, the inlet to the filter holder was replaced by a modified version having a longer cone, the inside half-angle being 15°. The modified, final version of the cyclone is shown in Figure 2.

☆Gelman Instrument Company, Ann Arbor, Michigan.

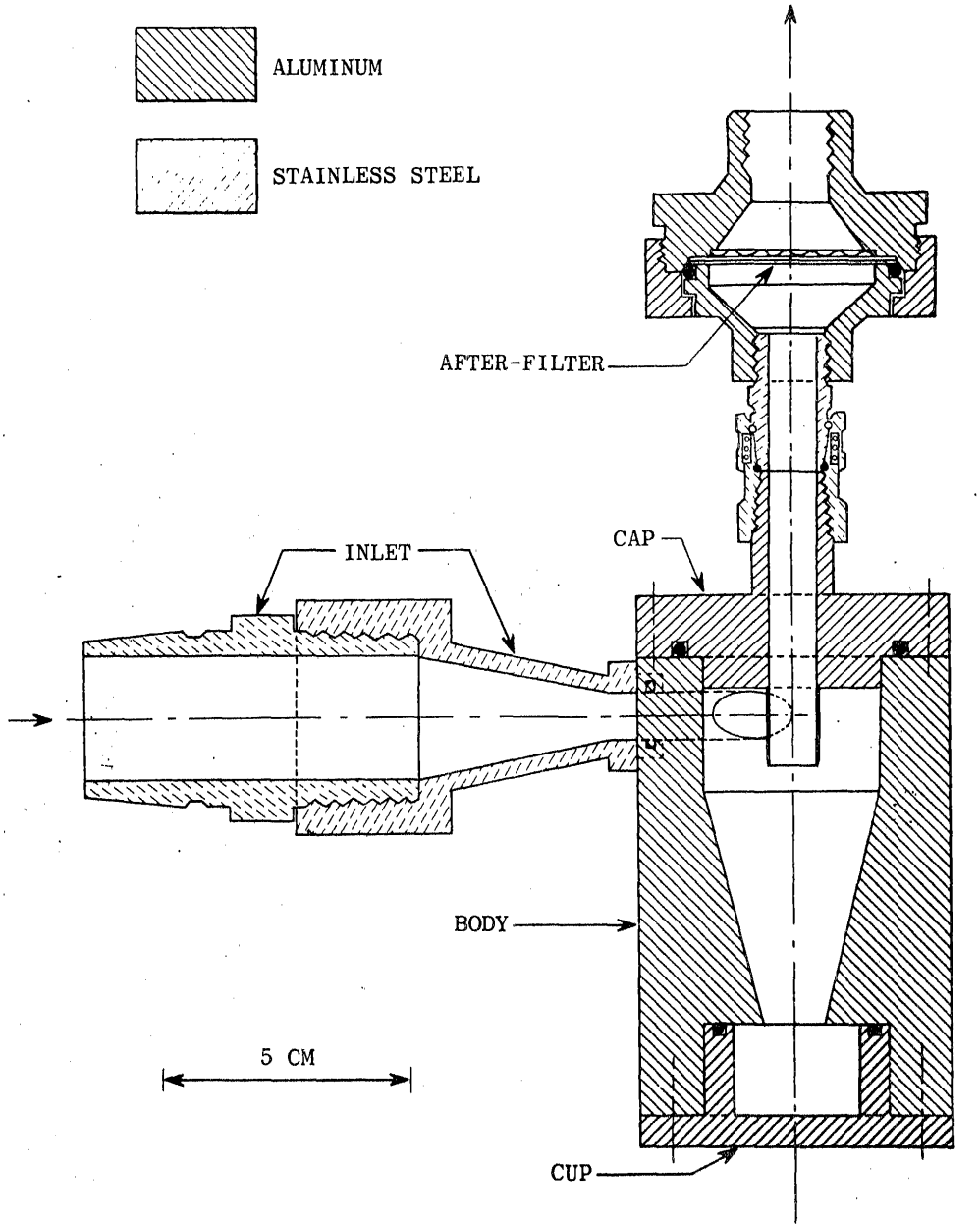

Figure 1

Assembly Drawing of the First Version of the Cyclone Sampler Developed for This Work

Table 1

CYCLONE DIMENSIONS

Inlet pipe diameter	2.54 cm
Inlet cone taper	15°
Cyclone inlet diameter	1.008 cm
Cyclone cylinder diameter	3.658 cm
Cyclone cylinder height	1.173 cm
Total cyclone height	5.923 cm
Diameter of cone bottom	1.270 cm
Diameter of cyclone outlet	1.052 cm
Length of outlet inside cyclone	1.570 cm

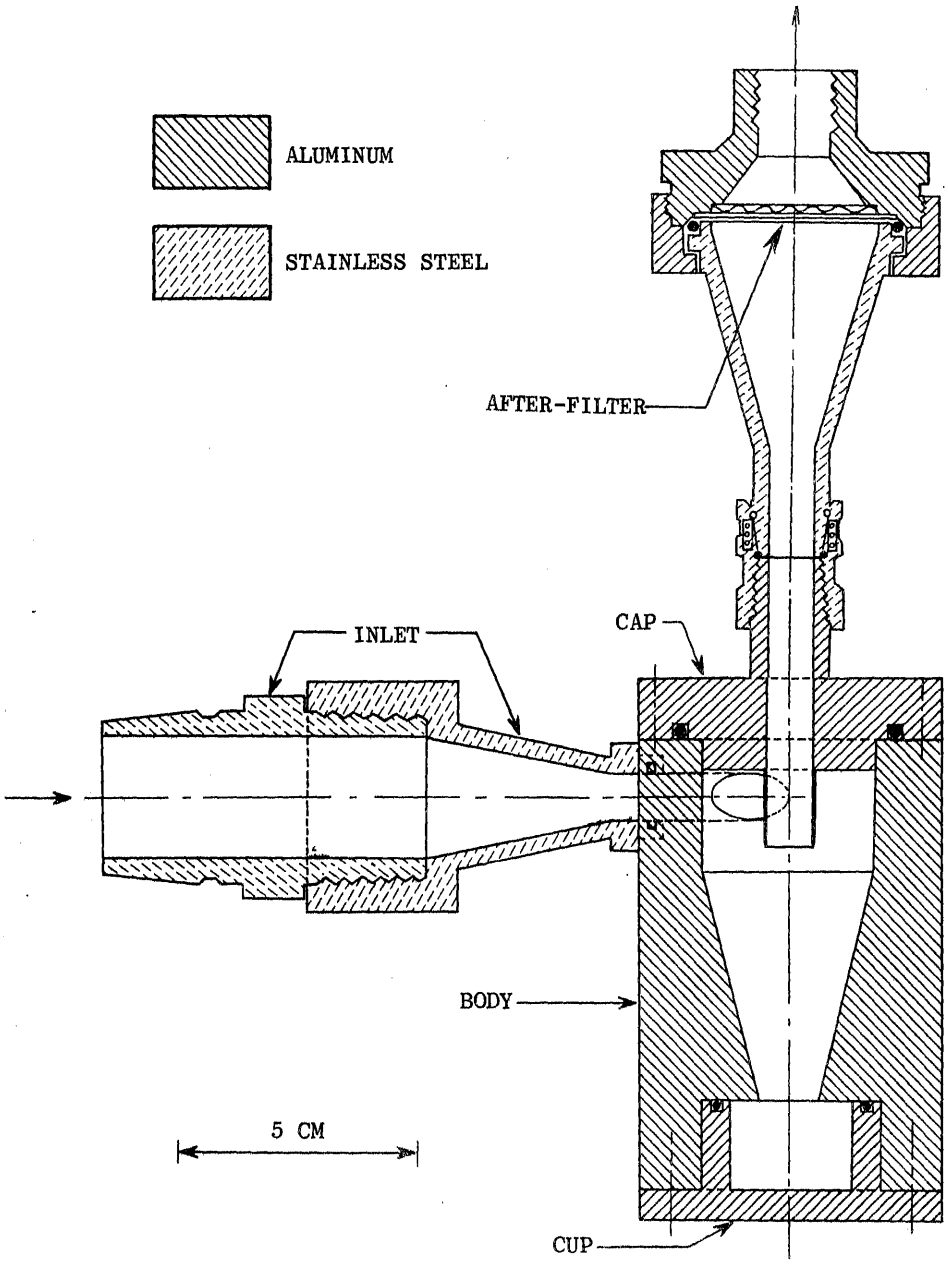

Figure 2

Assembly Drawing of the Second Version of the Cyclone Sampler with the Modified Filter Inlet.

The cyclone after-filter receives the fine fraction, particles smaller than about 3.5 μm, the 50% cut point. The coarse fraction, particles larger than the cyclone cut point, can be determined indirectly by sampling in parallel with a total filter, and subtracting the fine fraction from the total. It is important that the cyclone and total filter samples be obtained under nearly identical conditions. A sampler assembly designed to accomplish this is shown in Figure 3. The assembly was not constructed as part of the present project.

B. Tests on cyclone sampler

The test program was designed to be unusually thorough in order to provide definitive data with which to evaluate the cyclone and because of uncertainties arising from the empirical nature of cyclone design. Previous work has shown the particle collection characteristics to depend on whether the air flow is laminar or turbulent.[20]

It has been suggested that whether or not a vortex is established in the outlet flow depends on cyclone geometry and the flow rate.[21] The air flow characteristics can be most simply investigated by measuring the pressure drop across the cyclone as a function of flow rate.

Test data which have been obtained include the pressure drop across the cyclone as a function of flow rate, the fraction of particles deposited on the after-filter as a function of flow rate and particle size, and the dependence of the 50% cut point as a function of flow rate. Measurements were made of the deposition of both solid and liquid particles in the various components of the cyclone. Tests were conducted on the fraction of particles deposited in the cyclone which subsequently became reentrained.

1. Pressure drop measurements

The pressure drop across the cyclone was measured with clean

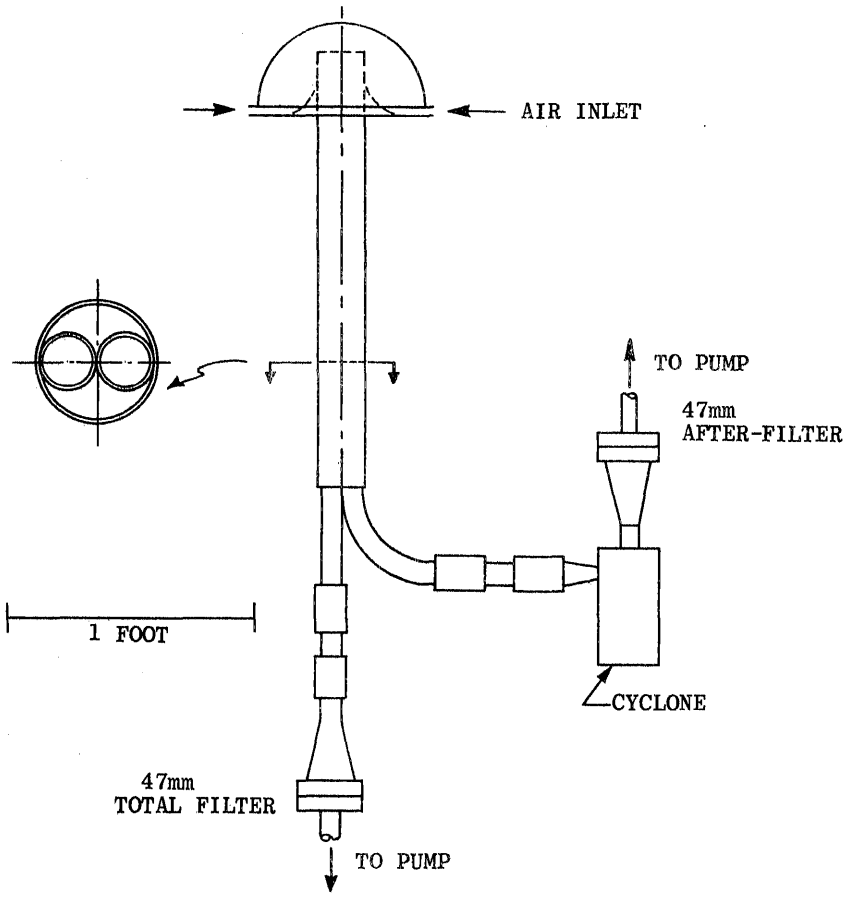

Figure 3

Assembly for Sampling with a Total Filter and Cyclone in Parallel

air at ambient pressure entering the inlet and a pressure gauge at the outlet replacing the filter assembly. The observed pressure drop vs. flow rate is shown as a log-log plot in Figure 4. The straight line fitting the data indicates that the pressure drop Δp is proportional to $Q^{2.60}$, where Q is the flow rate. At the normal operating flow rate of the cyclone (ca. 15 ℓ/min.), the pressure drop is only 0.03 cm Hg (0.16 in H_2O). These results are qualitatively similar to those obtained by others.[21,22] However, it is noteworthy that this cyclone does not exhibit any instabilities accompanied by shifts of the pressure-flow rate curve. Such shifts have been interpreted as indicating that the air flow changes from laminar to turbulent.[21] We conclude that our cyclone operates entirely in one flow regime in accordance with observations by Ayer and Hochstrasser[21] on cyclones with relatively short cones.

2. Cyclone deposition efficiency measurements

As a first step in the calibration of the cyclone with laboratory aerosol, the efficiency for deposition of particles on the after-filter was measured as a function of flow rate and particle size. The experimental arrangement is illustrated in Figure 5. Monodisperse methylene blue particles were generated by a Berglund-Liu vibrating orifice aerosol generator[23], electric charges on the particles were neutralized with a Kr-85 radioactive source, and gaseous ions created by the radiation were swept out of the gas by a transverse electric field. The aerosol accumulated in a plenum where the concentration and size distribution was monitored by a Climet optical particle analyzer.

The efficiency for deposition on the after-filter was obtained by first measuring the total deposition on a filter as shown in Figure 5, then replacing the filter holder with the cyclone assembly and measuring the deposition on the after-filter. The

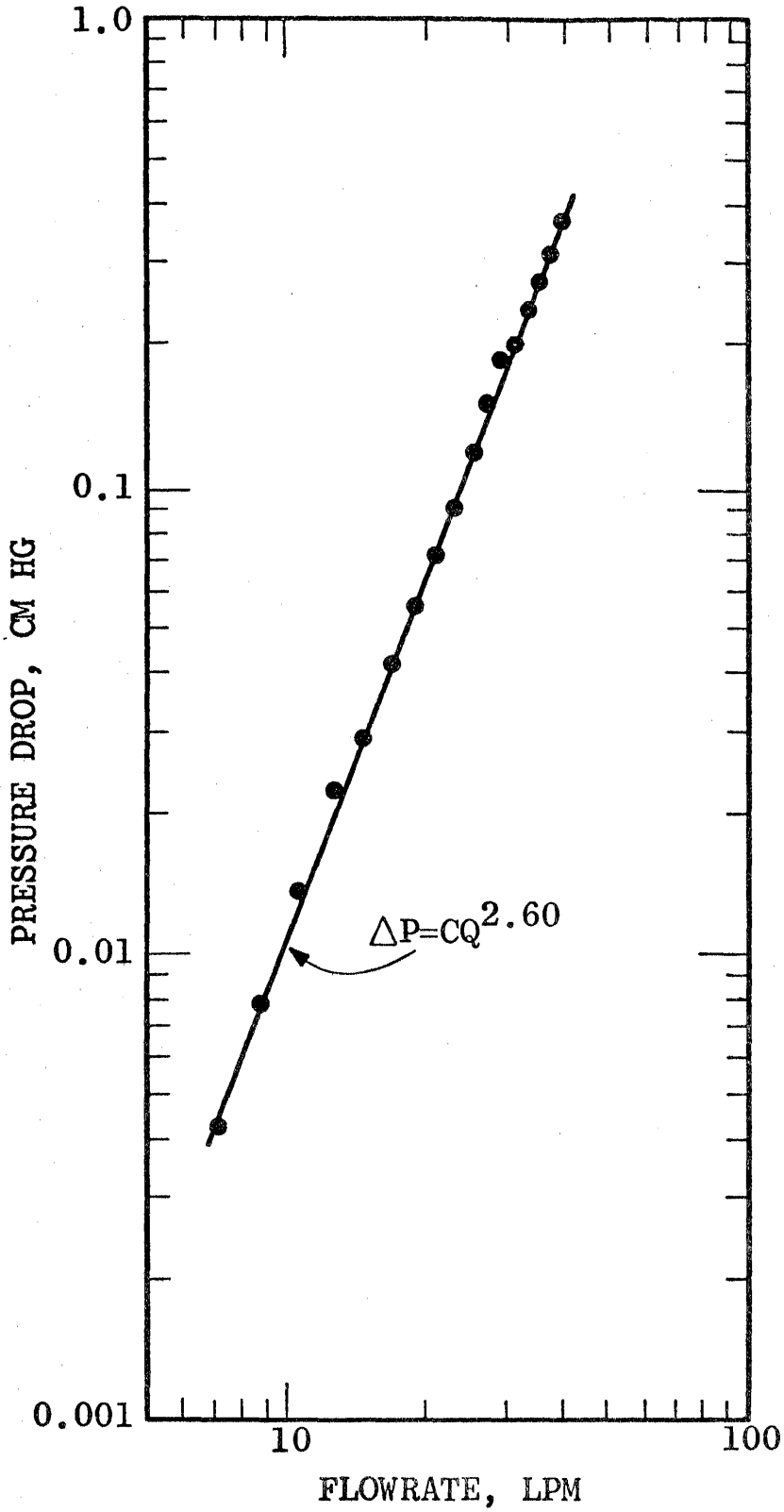

Figure 4

Pressure Drop Across the Cyclone
(Not Including the After-Filter)
As a Function of the Flow Rate

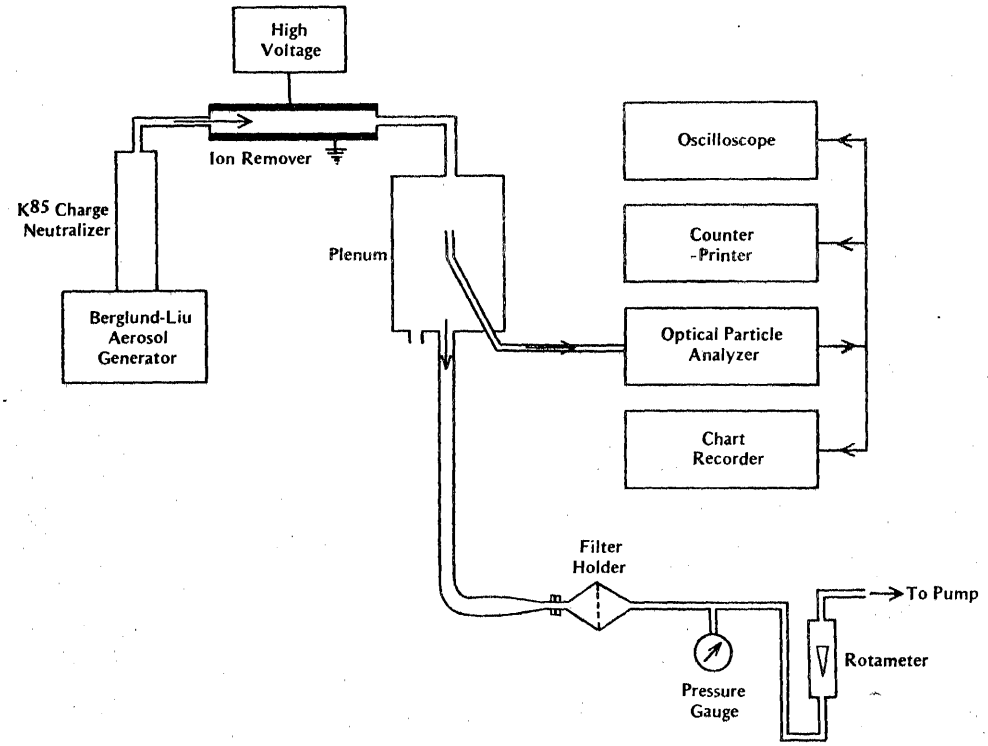

Figure 5

Experimental Arrangement for Tests with Laboratory Aerosol. After Measurement of the Aerosol Concentration, the Filter Holder is Replaced with the Cyclone Assembly

ratio of the particle mass on the after-filter divided by the mass on the total filter gives the efficiency. The particle mass was determined by dissolving the 0.8 μm pore size Millipore filters (cellulose acetate membrane) in acetone and quantitating the methylene blue on a Bausch and Lomb Spectronic 20 spectrophotometer operated at 610 nm wavelength. Since the two filter samples were taken at different times, a correction is necessary for small changes in particle concentration of the test aerosol with time. This was done on the basis of the Climet counts taken during the filter exposures. Because the rotameter is at reduced pressure, the flow rate was corrected using the measured pressure. It was necessary to correct each run since the pressure drop across individual membrane filters varies somewhat.

Results for the fraction of particles deposited in the cyclone as a function of particle size are plotted in Figure 6. The curves are progressively steeper as the flow rate is increased. At 15.4 ℓ/min. where the 50% cutoff diameter is 3.5 μm, the ratio D_{90}/D_{10} is 1.95 (the subscripts denote the percentage deposited). This is about the same as the D_{90}/D_{10} value $\sim$ 1.9 for the first stage of the Multi-day impactor[☆]. Thus, the sharpness of the cutoff characteristic is comparable to that of a cascade impactor.

The 50% cutoff diameters for each flow rate can be read from the curves in Figure 6. These are plotted in Figure 7 on a log-log plot. The line fitting the points gives the dependence of D_{50} on flow rate as

$$D_{50} = CQ^{-0.97}$$

where C is a constant. The values of the exponent which have

[☆]Sierra Instruments, Carmel Valley, CA.

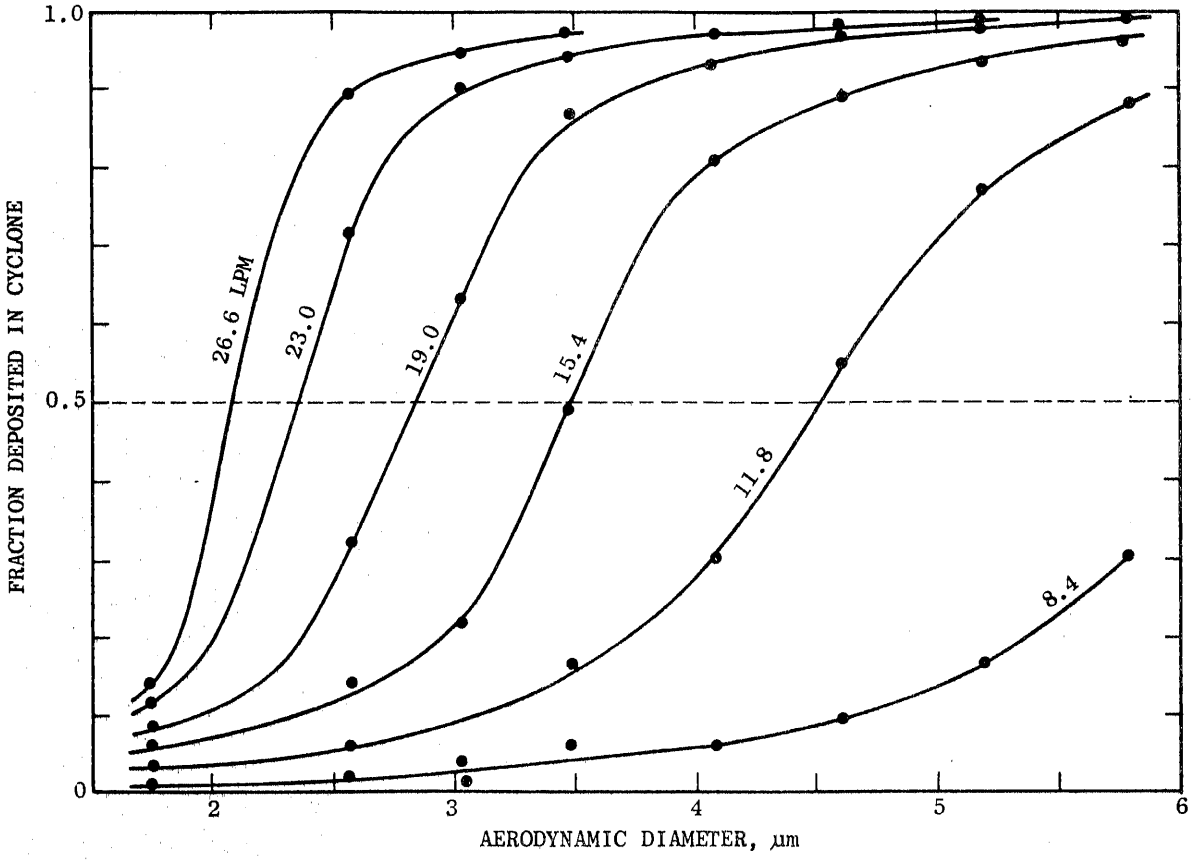

Figure 6

Fraction of Methylene Blue Particles Deposited in the Cyclone as a Function of the Aerodynamic Particle Diameter. The Curves are Labelled with the Flow Rate.

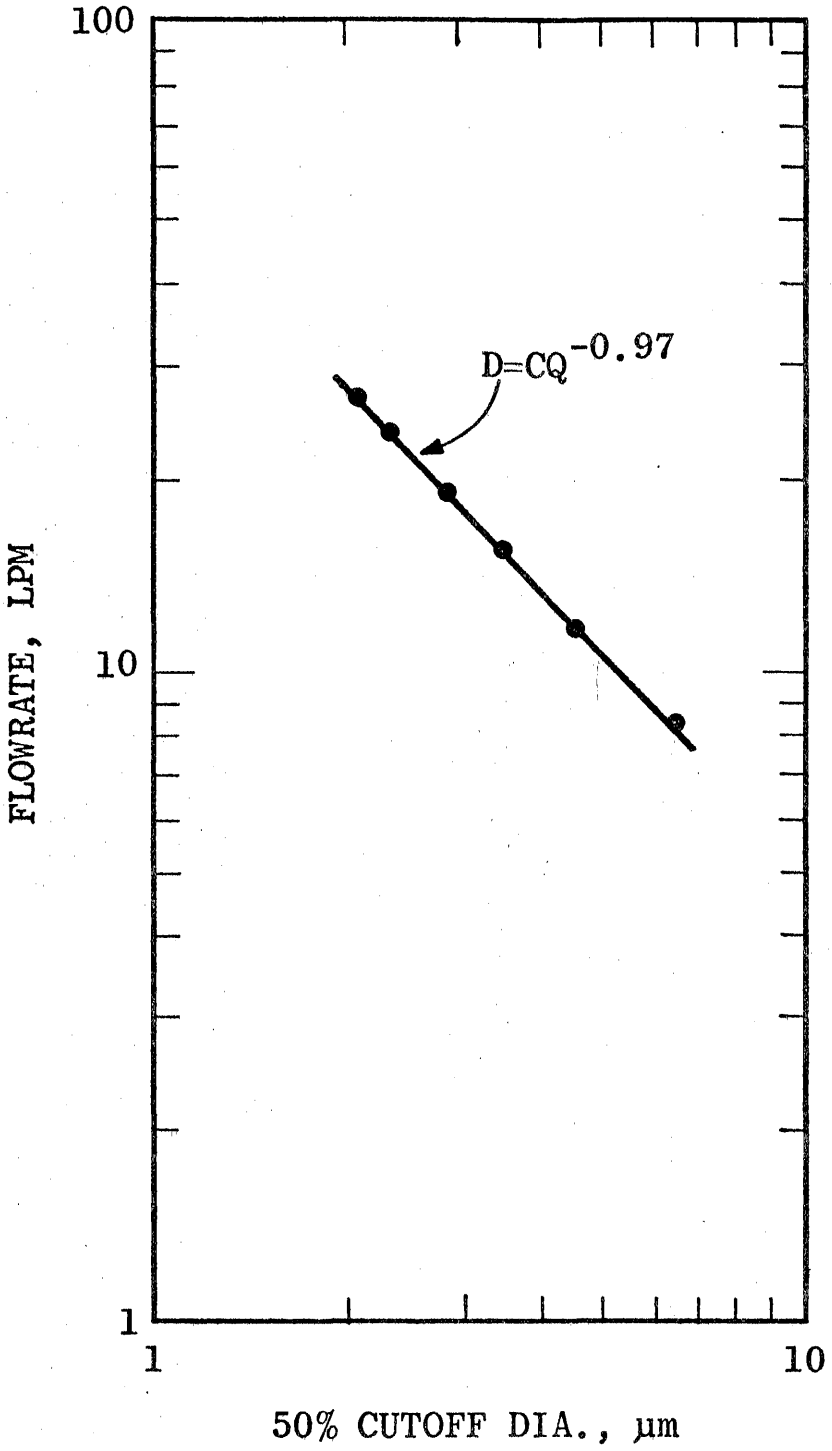

Figure 7

50% Cutoff Diameter of the Cyclone as a Function of Flow Rate from Measurements with Methylene Blue Aerosol

been obtained by others vary from 0.5 to about 1.5.[22,24] The value of 0.5 is typical of the large dust cleaning cyclones. The smaller cyclones operated at reasonably high flow velocities have exponents near 1.0. Bernstein, et al.,[24] have observed a break in the D_{50} vs. Q curve for the Dorr-Oliver cyclone with the exponent changing abruptly at 5 ℓ/min. Earlier experiments by Blachman and Lippmann[20] found that the particle retention characteristics changed at 5 ℓ/min. where the Reynolds number at the inlet becomes greater than 2000. The Reynolds number at the inlet of our cyclone varies from 950 to 3000 over the range of flow rate investigated, 8.4 to 26.6 ℓ/min. However, Figure 5 again shows that the cyclone is operating in one flow regime.

3. Detailed study of particle deposition in the cyclone
The purpose of this study was twofold, to compare the deposition efficiencies for solid and liquid particles, and to determine the relative amounts deposited in the various parts of the cyclone. Both quantitative and qualitative (visual examination) observations were made. The comparison of solid particles (methylene blue) and liquid particles (DOP) can reveal possible differences in retention of bouncy vs. sticky particles. Such differences would be important in the sampling of ambient air where, for example, soil-derived particles tend to be dry and bouncy whereas urban aerosols tend to be sticky. For these studies, the cyclone was operated at 15.4 ℓ/min. which, as we have seen, gives a D_{50} of 3.5 μm for methylene blue particles. The deposition was determined in four parts of the cyclone, the body, the cup, the cap (including the outlet tube) and the after-filter. These parts are labelled in Figure 1.

Monodisperse particles ranging from 1.5 to 7.6 μm aerodynamic diameter were produced by the Berglund-Liu generator. After a timed exposure to methylene blue aerosol, the cyclone was

disassembled and the parts except for the after-filter were washed with 50% isopropyl alcohol-50% water solution. The Millipore filter was dissolved in acetone which also dissolves the methylene blue. It was determined that the presence of acetone and/or cellulose acetate did not affect the spectrophotometer's response to methylene blue.

For production of oil particles, DOP (dioctylpthalate) was dissolved in 85% isopropyl alcohol, 15% water with disodium fluorescein (5% of the DOP vol.) added as a tracer. After sampling, the cyclone parts were washed with the same solvents and quantitated with a Turner Fluorometer. Cellulose acetate filters could not be used for DOP-fluorescein particles since it was found that both acetone and the filter material quenched the fluorescence by up to an order of magnitude. A satisfactory alternative was found in the use of Fluoropore membrane filters (Teflon). Filter samples were washed and sonicated in isopropyl alcohol. Tests showed the extraction to be complete; the particles do not adhere strongly to the Teflon.

The results are shown in Figure 8. Perhaps the most important result is the close agreement between the methylene blue and DOP curves for deposition on the after-filter. The differences are, in fact, barely experimentally significant. Thus, the cyclone samples solid and liquid particles with essentially the same efficiency. Both curves show that loss of particles in the cyclone becomes negligible below 2 μm.

For methylene blue particles, deposits within the cyclone are greatest in the cup, followed by deposits on the body. The latter increase with particle size as expected from inertial impaction. Deposits on the cap are less than 5% over most of the range. DOP particles have a similar deposition pattern when the particle size is less than the D_{50} of 3.5 μm. Above

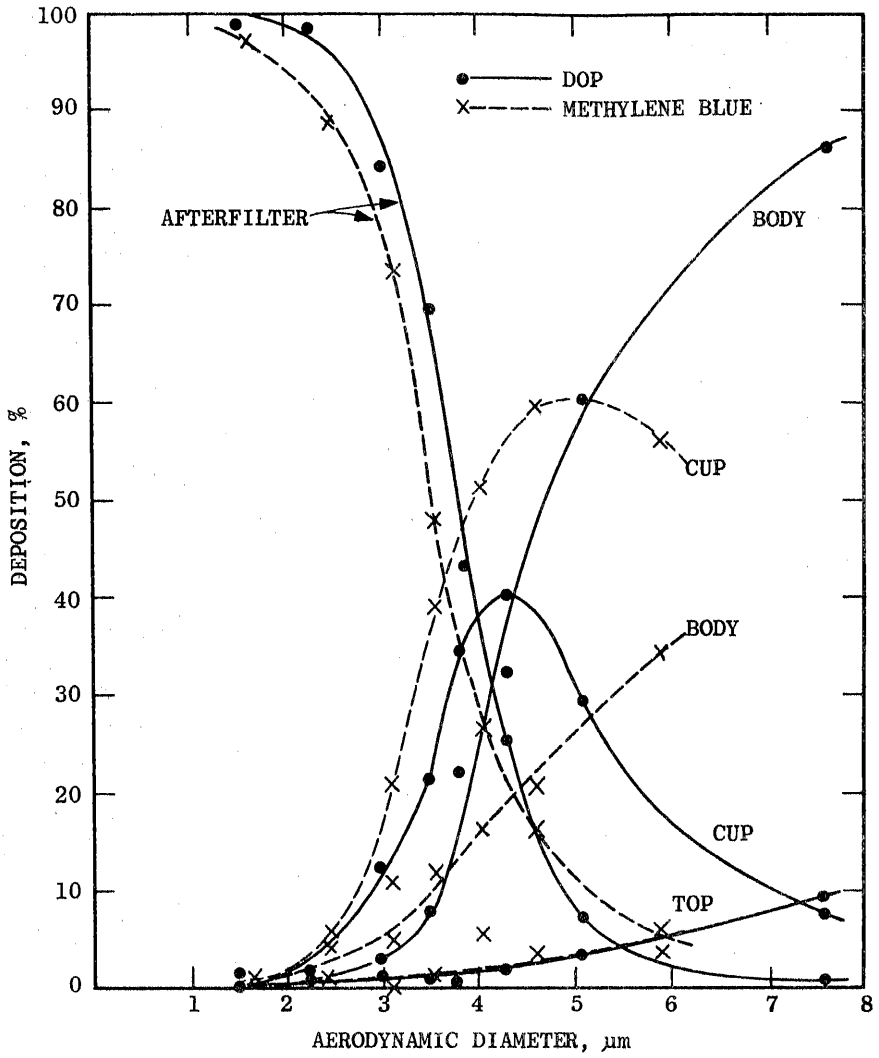

Figure 8

Percentage of Particles Deposited on the Various Components of the Cyclone Sampler vs. the Aerodynamic Particle Diameter, Flow Rate 15 ℓ/min.

3.5 μm, the deposition on the body rapidly becomes dominant. Evidently, almost half of the large methylene blue particles strike the wall but either rebound or slide into the cup. Alternatively, some particles form aggregates on the walls of the body and then detach to fall into the cup.

The percentages of particles deposited in the cyclone parts excluding the after-filter are plotted in Figure 9. This plot emphasizes the competition between the body and cup. Thus far, the data discussed have been from runs involving a total deposit of about 130 μg. Three long runs were made using methylene blue with total deposits of 2.3 to 4.5 mg. These points, shown in Figure 9, show decreased deposition on the body and increased deposition in the cup. Thus, aggregates tend to fall from the wall of the body to the cup.

Deposits on the inlet were also measured. Over all particle sizes, deposits averaged 0.9% and 1.4% of the total for DOP and methylene blue, respectively. Deposits on the housing of the after-filter were negligible.

Valuable information on the details of the cyclone performance was also obtained by visual observation of the methylene blue deposits. The following features were noted:

a. There is an impaction spot on the wall of the body opposite the inlet but not quite in a direct line. The amount of methylene blue is a small fraction of the total.

b. Two curved traces lead away from the impaction spot, one spirals upward against the lower surface of the cap, ending at the juncture with the outlet tube. The other trace spirals downward, becoming very steep on the tapered wall of the cone. The bottom is reached in 1.25 to 1.5 turns.

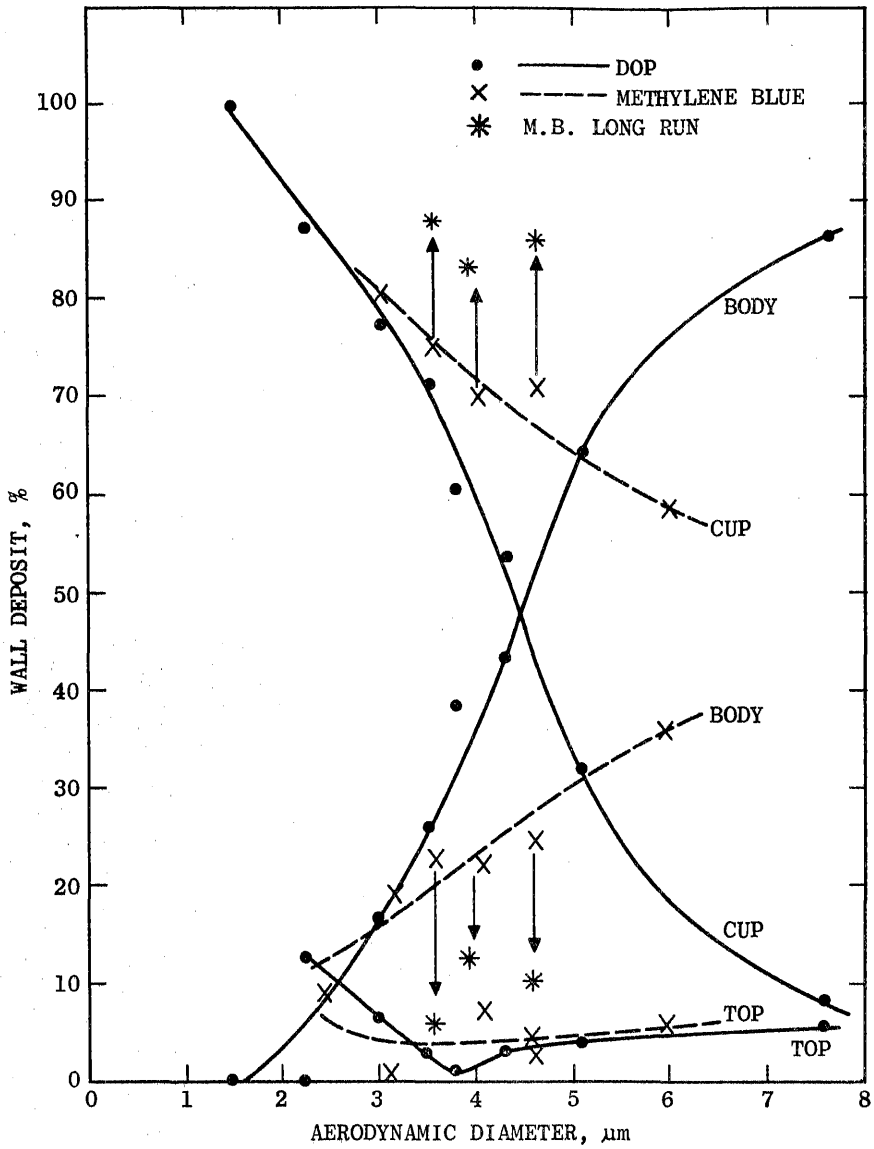

Figure 9

Percentage of Particles Deposited on the Cyclone Parts Excluding the After-Filter. The Arrows Indicate the Shift in Methylene Blue Deposition with Increased Loading.

c. The generalized deposit on the cone walls increases in density toward the bottom. As the density increases, aggregates become increasingly prevalent.

d. The cup deposits include large aggregates. The increasing deposit of particles with radial distance suggests the presence of a vortex even within the cup. Deposits on the lower surface of the body (which forms the roof of the cup) indicate the presence of eddies within the cup.

e. A spiral trace within the outlet tube is clearly visible, indicating a vortex within the tube.

4. Uniformity of the particle deposit on the after-filter

All of the above measurements were made with the cyclone configuration shown in Figure 1 wherein the after-filter holder was the Gelman Model 1235 which has a wide angle inlet. It was found that the methylene blue was not deposited uniformly on the filter. In order to improve the deposition, the inlet cone to the filter was replaced with a longer cone having a 15° half-angle as shown in Figure 2. The particle density was scanned with a microscope densitometer equipped with a precision x-y stage. Maps of the particle density on the filters taken with either the short or long cones for methylene blue particles having aerodynamic diameters of 2 μm, 3.5 μm and 4.5 μm are shown in Figure 10. The patterns for the short cone suggest that the vortex affects the particle deposition. With the long cone, the deposition is seen to be more uniform. Uniformity of the deposit is important if the filter is to be divided for a number of analyses. To assess the uniformity, we divided the area into 7.5 mm squares (roughly 1/15 of the total area) and calculated the standard deviation of the deposits. The results are listed in Table 2. For the long cone, the standard deviation is about 1% for particles smaller than the cut point.

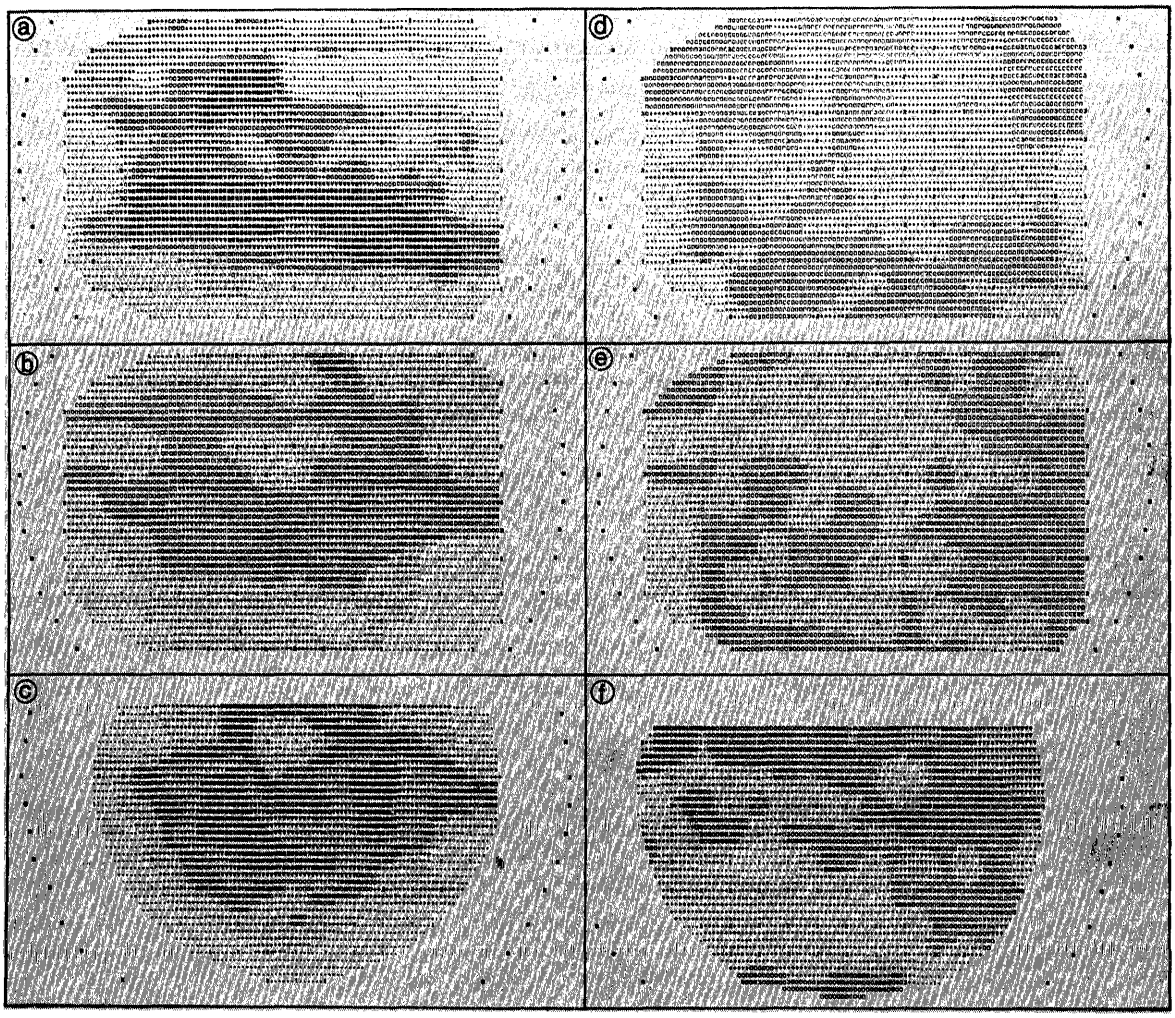

Figure 10

Maps of Particle Density on the After-Filter Made with Methylene Blue Particles and Either the Short or Long Inlet Cone on the Filter Holder

a. Short cone, 2 μm dia. particles.
b. Short cone, 3.5 μm dia. particles.
c. Short cone, 4.5 μm dia. particles.
d. Long cone, 2 μm dia. particles.
e. Long cone, 3.5 μm dia. particles.
f. Long cone, 4.5 μm dia. particles.

Table 2

STANDARD DEVIATIONS OF PARTICLE DEPOSITS
ON 7.5 mm x 7.5 mm AREAS OF THE AFTER-FILTER

Aerodynamic Diameter, μm	Short Cone Std. Dev., %	Long Cone Std. Dev., %
4.5	2.9	4.6
3.5	5.0	0.9
2.0	12.0	1.5

A check was made to determine if the modification of the inlet cone to the filter holder affected the cyclone aerodynamics. This consisted of measuring the pressure drop across the cyclone with the filter holder in place but with no filter in the holder. No difference was seen between the results with the short or long inlet cones. Also, no instability was seen. Therefore, the long inlet cone was adopted for the final version of the cyclone sampler.

5. Reentrainment studies

Reentrainment refers to the resuspension of particles which have been deposited within the cyclone. The reentrainment with which we are concerned is that which results in the deposition of the resuspended particles on the after-filter. This could alter the efficiency of the cyclone, especially under conditions of heavy loading. Reentrainment could result from the continuing flow of air over the deposits. It could also result from the impaction of particles onto the deposits, thereby dislodging particles, or a scouring effect.

Several experiments were conducted to investigate reentrainment. Test I was designed to detect reentrainment caused by air flow alone. The cyclone was loaded with 2.3 mg of 4.70 μm (aerodynamic diameter) methylene blue particles. This load is the mass equivalent of several days of ambient air sampling. The after-filter was replaced, and clean, dry air sampled at 15.4 ℓ/min. for one hour. This after-filter accumulated 0.0012 mg of methylene blue, or 0.05% of the cyclone loading in one hour. In 24 hours of sampling, this would be 1.2% reentrainment from air flow.

Test II was devised to include reentrainment caused by the impingement of particles. Loading with methylene blue was followed by sampling ambient air. First, a background check was made with a clean cyclone since ambient dust is not

colorless. The filter deposit from sampling ambient air for one day gave a reading on the spectrophotometer equivalent to less than 8 μg of methylene blue. The cyclone was then loaded with 2.1 mg of methylene blue particles with an aerodynamic diameter of 3.9 μm. The cyclone was then set up at an open window and run for 10 min. to eliminate any particles which might have been dislodged during the movement of the cyclone. With a clean after-filter, the cyclone was then operated at 15.4 ℓ/min. for 18.5 hours in the ambient air. The after-filter was then found to have 0.012 mg of methylene blue, or 0.57% of the cyclone loading equivalent to 0.73% reentrainment in 24 hours of sampling. This is an upper limit since an appreciable fraction of the spectrophotometer reading could come from the color of the ambient dust. It also represents an extreme test since normally the cyclone would be operated with an inlet which would exclude particles greater than ca. 20 μm diameter. After the test, the cup was found to contain particles up to 1000 μm in size. Such large particles would impact the cyclone wall with considerable momentum. Test II was repeated with 2.9 μm methylene blue particles with almost identical results. The very low reentrainment probability observed here (less than 0.7% of the load per day) may be explained by the operating mechanism of the cyclone. When a particle is deposited on the wall, it has left the vortex and entered the relatively stagnant boundary layer. If the particle becomes resuspended, it settles through the boundary layer, thus drifting down the walls and eventually into the cup. The deposition data taken with increasing loadings of methylene blue show just this behavior.

6. Sampling of ambient air

The cyclone was operated at 15.4 ℓ/min. for one week at the Bay Area Air Pollution Control District monitoring station in San Jose. The cyclone sampled isokinetically from a large

inlet manifold originally used in the ACHEX study.[10] The after-filter was changed daily. At the end of the week, the cyclone was taken apart for visual inspection. The patterns of the deposit were similar to those observed with methylene blue particles. The impaction point opposite the inlet was somewhat more heavily coated, indicating a more sticky aerosol. The spiral patterns were again clearly visible. The deposits had the typical fuzzy appearance of ambient dust, and large particles were found in the cup. No operational problems were encountered.

C. Summary of cyclone tests

A cyclone after-filter sampler has been constructed which is suitable for ambient air size-selective monitoring. It has been extensively evaluated with monodisperse laboratory-generated aerosol and subjected to preliminary testing in the atmosphere. The cyclone has been found to operate in the classical manner with a vortex in the cone and a vortex in the outlet flow. The dependence on flow rate of the pressure drop and the 50% cut point indicate a single flow regime over the range investigated. At 15.4 ℓ/min. the D_{50} is 3.5 μm. The cutoff characteristic curve is comparable to that of a cascade impactor and is the same for solid or liquid particles.

Reentrainment of previously deposited particles is less than 1% of the loading per day. No operational problems were encountered in preliminary field operation. On the basis of all of these tests, this cyclone appears to be a very satisfactory size-selective sampler.

IV. TESTING OF A DICHOTOMOUS VIRTUAL IMPACTOR

Samplers utilizing the virtual impaction principle[25,26] were devised to avoid the bounceoff problem inherent in the conventional cascade impactor. As implied by the name, the dichotomous virtual impactor[6,27,28] separates the particles into two size fractions. The dichotomous virtual impactor was expressly developed so that the samples could be analyzed by x-ray fluorescence. The present testing was performed on the Sierra Instruments Model 243 Virtual Impactor, the only commercially available sampler of this type. This is essentially the same sampler as one previously marketed by the Environmental Research Corporation (ERC). A description of the ERC sampler and a calibration curve was presented by Dzubay, et al.[6] The sampler should not be confused with an earlier ERC model having a different stage design which was tested by Loo and Jaklevic.[29]

The Sierra dichotomous virtual impactor is shown in Figure 11. At the first stage, most of the air stream turns 90° through the annular gap, taking the fine particles with it. The coarse particles, because of their inertia continue down to the next tubular section with approximately 1/6 of the air flow. However, this small air flow also carries with it 1/6 of the fine particles since they follow streamlines. In order to improve the separation of the particles into two size fractions, a second stage is added. The fraction of small particles carried over into the coarse fraction is then reduced to 1/6 x 1/6 = 1/36. The coarse fraction and the fine fractions are collected onto two separate 37 mm diameter filters as shown. Membrane filters such as Fluoropore can be employed for 24-hour sampling of ambient air. Additional details can be found in Reference 6.

The sampler was pumped by a dual mass flow controller (Sierra Instruments). These flow controllers maintain a constant mass flow rate independent of

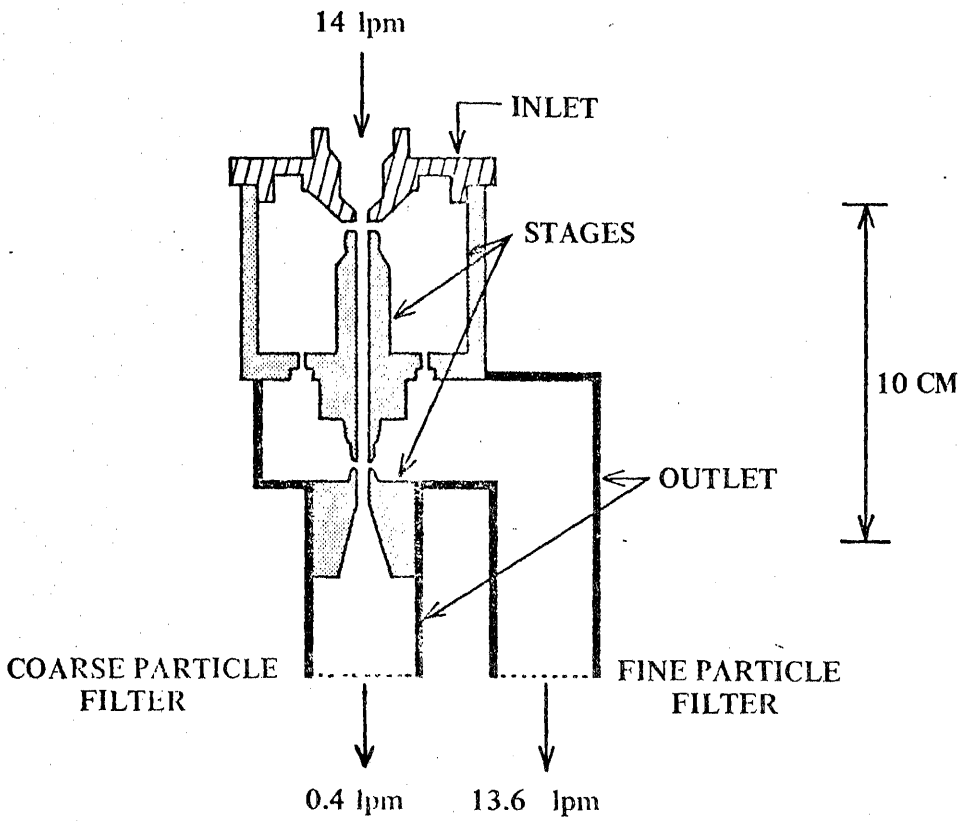

Figure 11

Schematic Drawing of the Dichotomous Virtual Impactor Tested

filter loading over a wide range by means of temperature sensors and feedback control. The manufacturer's specified total flow rate is 14 ℓ/min. We have made tests at three different flow rates, maintaining the ratio of the fine to coarse fraction flow rate constant at 38:1. (Coarse fraction flow rate is 1/39 = 2.56% of the total) This is only slightly different than the manufacturer's quoted ratio of 36:1. The flow rates are tabulated in Table 3. The filter holder supplied with the sampler was unsatisfactory because the support screen was not flush with the holding ring, resulting in cracked filters. A modified holder was designed to correct this problem. An O-ring was added to the holder to provide a positive seal.

A. Particle deposition in the dichotomous virtual impactor

The experimental techniques used to measure particle deposition were the same as those used for testing the cyclone. For wall loss measurements, the sampler was disassembled and three separate sections washed with solvent. The three sections, denoted as inlet, stages and outlet are indicated in Figure 11.

1. Methylene blue deposition measurements

The deposition curves for methylene blue particles are shown in Figures 12-14 for total flow rates of 10.7, 14 and 20 ℓ/min. We define the cut point as the crossover point of the fine and coarse fraction curves. The individual fine or coarse particle 50% cut points differ from the crossover point by about 0.1 μm. The crossover cut points are listed in Table 3. We note that the 2.8 μm cut point for 14 ℓ/min. is smaller than the design value of 3.5 μm. Based on the three measurements, the dependence of the cut point on flow rate is fitted by

$$D_{\text{cut point}}(\mu m) = 8.8\ (Q,\ \ell/\text{min})^{-0.43}$$

The exponent is slightly smaller than 0.5, the value for a conventional impactor.

Table 3

FLOW RATES AND MEASURED CUT POINTS

Coarse Fraction ℓpm	Fine Fraction ℓpm	Total ℓpm	Cut Point* μm
0.28	10.45	10.73	3.2
0.36	13.64	14.00	2.8
0.51	19.49	20.00	2.4

*Aerodynamic diameter.

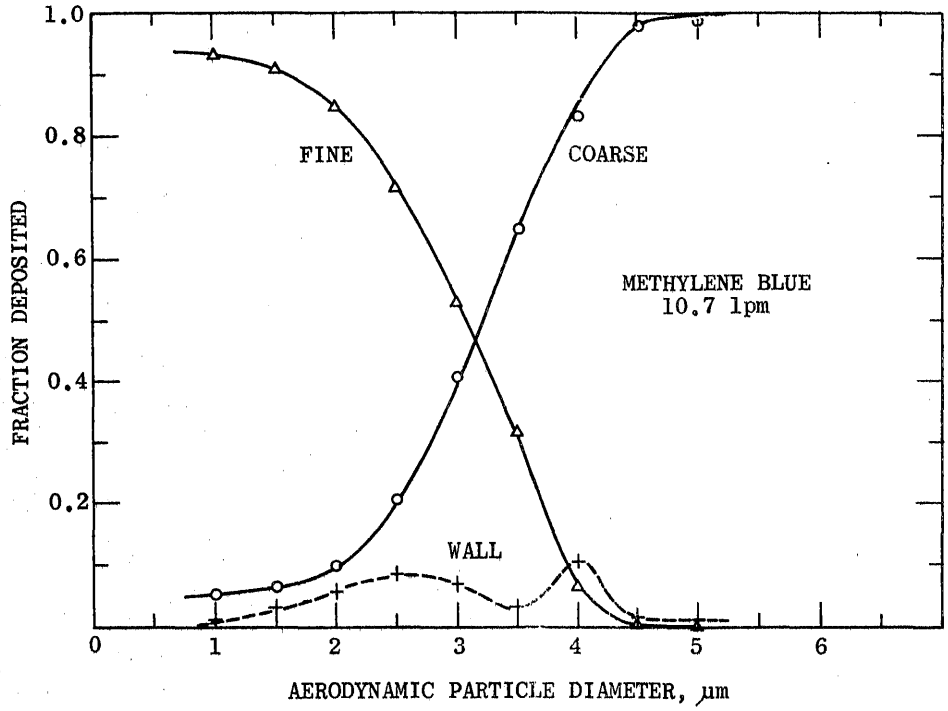

Figure 12

Fraction of Methylene Blue Particles Deposited on the Fine Filter, Coarse Filter and Wall vs. Particle Diameter at 10.7 ℓ/min. Flow Rate

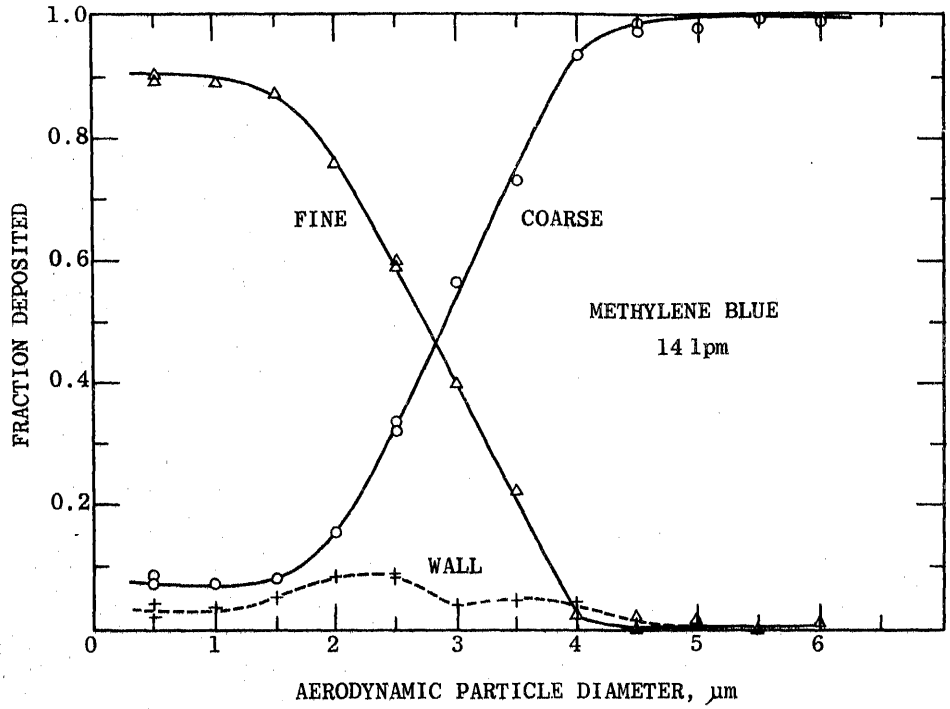

Figure 13

Methylene Blue Deposition at 14 ℓ/min Total Flow Rate

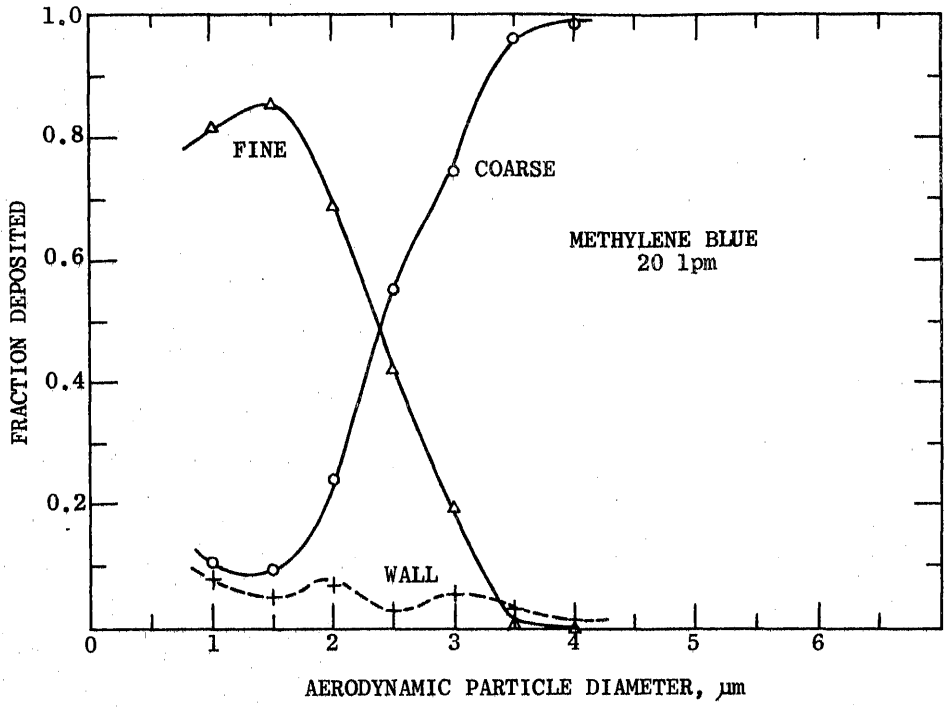

Figure 14

Methylene Blue Deposition at 20 ℓ/min Total Flow Rate

The sharpness of the cutoff is fairly independent of flow rate. The ratio of the particle diameter for 90% deposition to that for 10% deposition D_{90}/D_{10} is 2.2. For comparison, the AIHL cyclone has a D_{90}/D_{10} of 2.0, the Multiday[☆] impactor, 1.9. Above the cut point, the coarse fraction rises to 98-99% within 2 μm. Below the cut point, the fine fraction reaches values short of the ideal maximum of 97.4%, including the flow correction. The discrepancy is 1, 6 and 13% at 10.7, 14 and 20 ℓ/min., respectively. The loss from the fine fraction appears partly in the wall fraction and partly in the coarse fraction. At 20 ℓ/min., the coarse fraction is 10.3%, which is 7.7% larger than accounted for by the 2.6% due to the crossover air flow. This surprising experimental finding is difficult to explain. This effect has not been previously reported, but the measurements of Dzubay, et al.[6], did not extend below 2 μm.

The total wall loss, plotted in Figures 12-14, displays systematically two peaks, one slightly above and one slightly below the cut point. The maximum loss is less than 10%. The wall losses in the separate sections of the impactor are shown in Figures 15-17. The largest loss is on the stages and the second largest on the outlet. Inlet losses were negligible except for much larger particle sizes.

Visual examination of the methylene blue deposits revealed that by far the largest wall loss was incurred around the conical sides of the bottom tube of the second stage. Lesser losses were observed on the bottom tube of the first stage and the holes which conduct the fine fraction leaving the first stage. In interpreting the details of the data it is well to remember that the sampler has two stages which may not have exactly the same cut point.

2. DOP deposition measurements

The deposition curves for DOP-uranine shown in Figure 18, exhibit a curious structure. The curves for the fine and coarse fractions

[☆]Sierra Instruments, Carmel Valley, CA

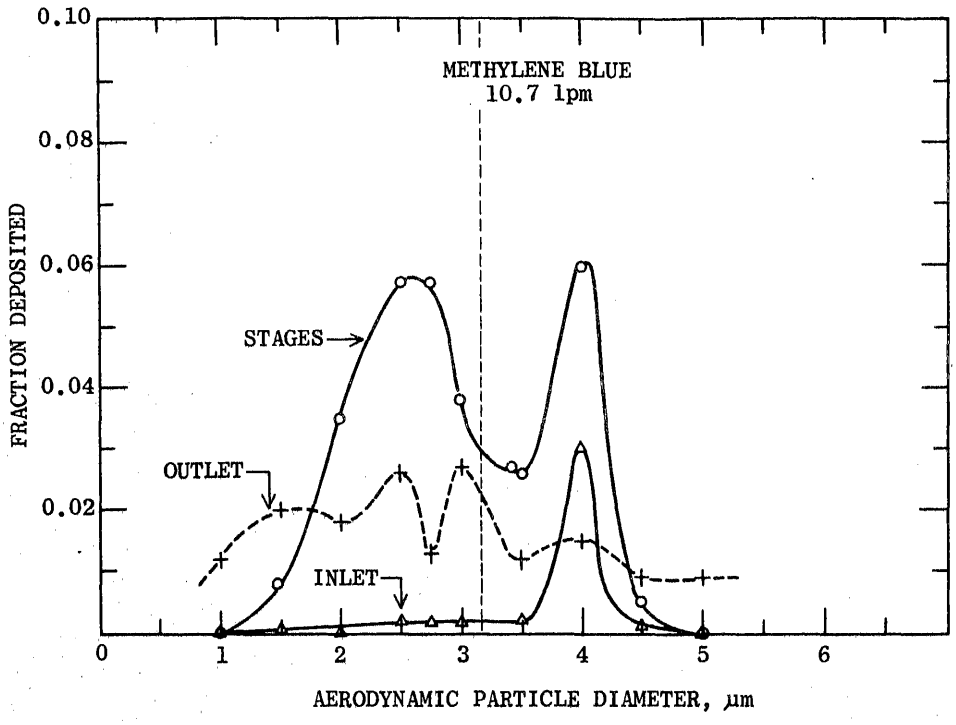

Figure 15

Wall Losses for Methylene Blue Particles
at a Flow Rate of 10.7 ℓ/min.

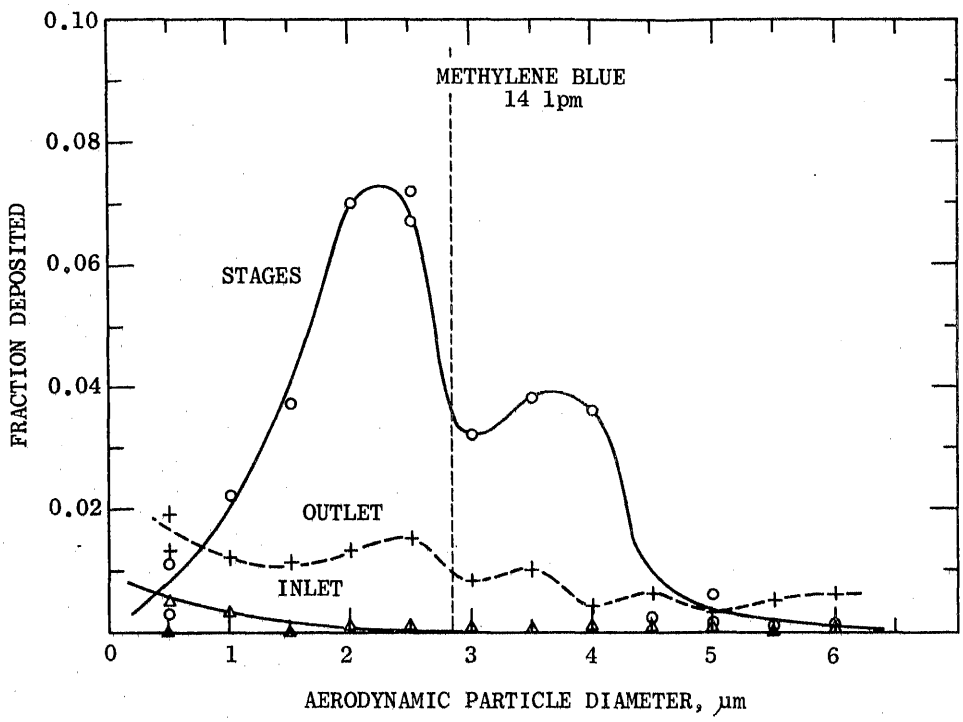

Figure 16

Wall Losses for Methylene Blue Particles
at a Flow Rate of 14 ℓ/min.

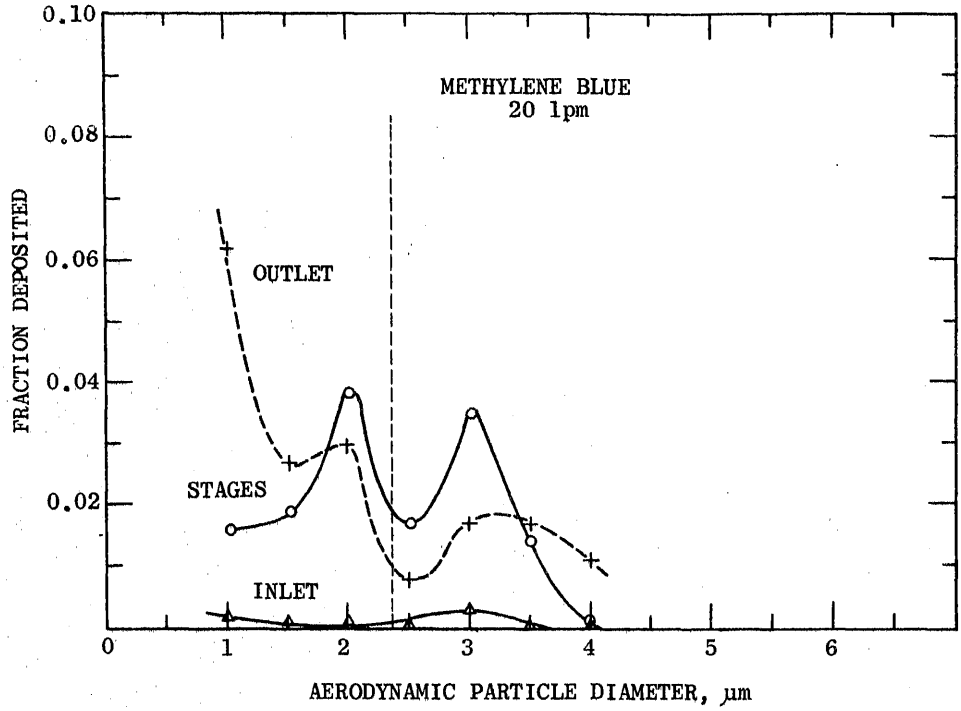

Figure 17

Wall Losses for Methylene Blue Particles
at a Flow Rate of 20 ℓ/min.

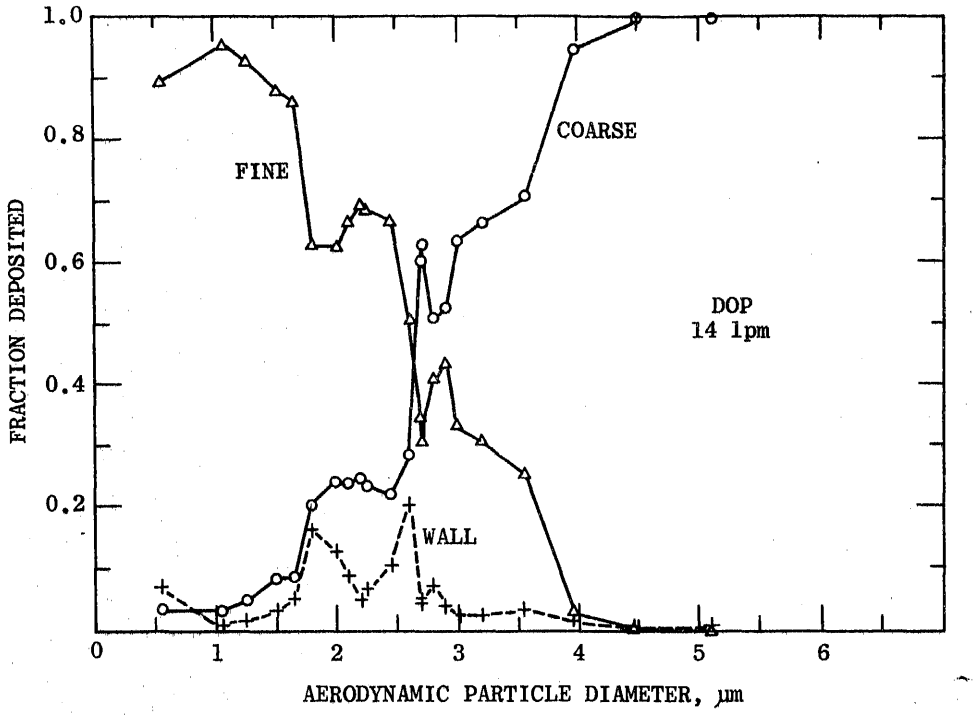

Figure 18

Fraction of DOP Particles Deposited on the Fine Filter, Coarse Filter and Wall at 14 ℓ/min.

oscillate around the corresponding curves for methylene blue particles. In Figure 19, the difference between the DOP and methylene blue deposition fractions is plotted vs. particle diameter. The difference is less than 20% throughout and the coarse and fine curves tend to be complementary. A possible explanation of the observed structure could be droplet breakup on the edges of the stage tubes. Fragments from a droplet may then be deposited on the "wrong" filter. It is necessary to mention a complication due to the structure of the DOP-uranine particles. Because uranine is insoluble in DOP, under the microscope the particle resembles a raw egg with an orange uranine "yolk" surrounded by clear DOP "white". The uranine "yolk" carries the tracer material which is detected. When the composite particle breaks up, it is likely that all of the uranine "yolk" will go to either the coarse or fine fraction filter. The net result may not be exactly the same as that from the breakup of a uniform particle.

Although structure in the deposition curves for a virtual impactor have not been reported previously, there exist no data with detail comparable to that presented here. Also, no such structure was seen in the cyclone tests so that it is unlikely to be an artifact of the measurement technique.

The fine fraction deposition for 0.5 μm DOP particles is 5.5% below the ideal 97.4%. This is similar to the effect noted for small methylene blue particles. However, for DOP the deposition is transferred mainly to the wall.

The total wall loss again exhibits two peaks, but both are below the cut point. The maximum is 20%, larger than for solid methylene blue particles as expected since liquid particles will tend to stick to the wall. In Figure 20, the wall losses on the separate sections of the sampler are plotted. Again, the major losses are on the stages. The total wall loss remained low between 5 and

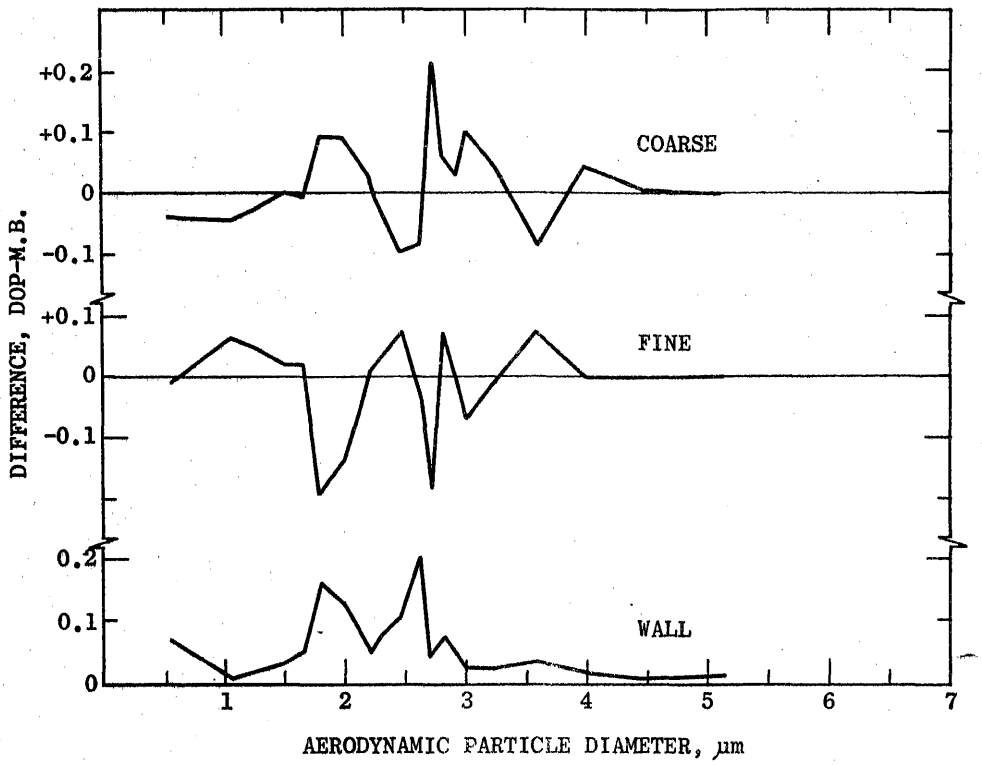

Figure 19

Differences Between the Deposition Fractions for DOP and Methylene Blue Particles vs. Particle Diameter. The Wall Loss for DOP is Plotted Directly.

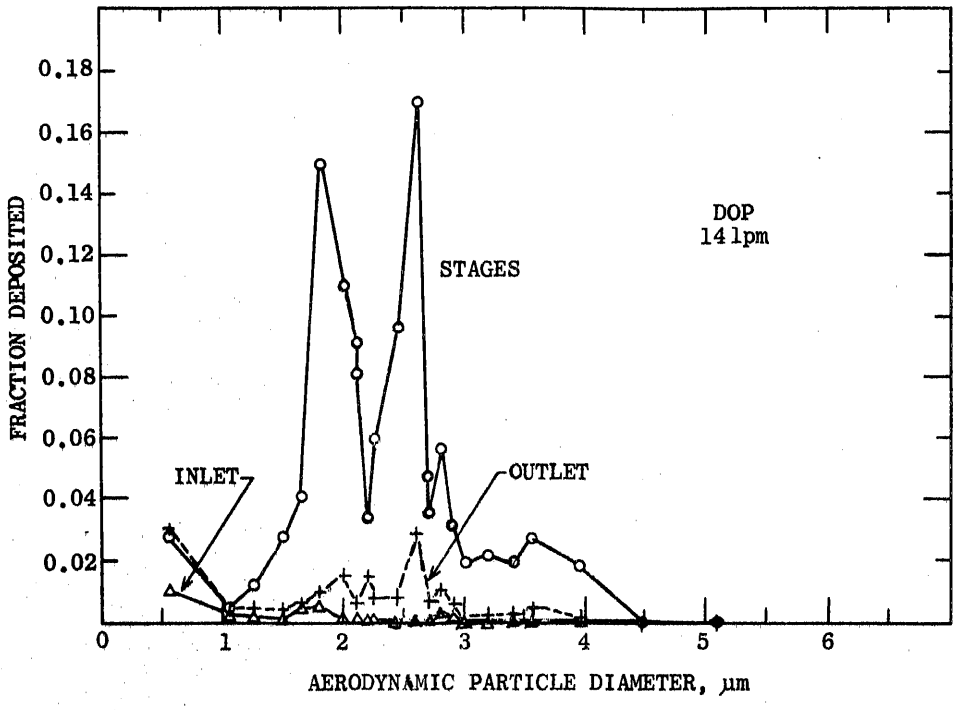

Figure 20

Wall Losses for DOP Particles

10 μm, and then jumped to 16.5% at 16.5 μm diameter (Figure 21). The large particles were lost in the inlet as expected.

3. Uniformity of the particle deposits on the filters

A selection of filters containing methylene blue particles were scanned with the microdensitometer. The readings were averaged over quarter sections of the 37 mm filter. Then the standard deviation of the four sections were computed. From the results listed in Table 4, it can be seen that the standard deviation is less than 10% for the filter containing the major fraction of the particles of the size in question. The other filter containing the minor fraction (less than 20% of the particles) shows large standard deviations. The non-uniformities were, in fact, readily apparent upon inspection. The non-uniformity of the minor fraction however, would ordinarily not be of concern in the sampling of ambient air.

4. Sampler inlet

The sampler is normally supplied with a directional inlet having a vane to orient the air intake into the wind. The bearing of this assembly was found to have excessive friction. It seems inherently difficult to construct a swivelling connection which has low friction and is also air-tight. Moreover, we are not convinced that this is a desirable type of inlet. Our preference is for a static intake with an annular inlet so that the sampling is independent of wind direction. The inlet should also be designed to have a definite cutoff for large particles so that the coarse fraction is defined. Another desirable feature, independence of wind speed, can only be approximated to some degree. We know of no inlet which has been demonstrated to satisfy all of the above requirements. Because of the imperfect state of the art, we can only state our preference for a static inlet. Sierra Instruments has recently made available a static inlet for the dichotomous sampler.

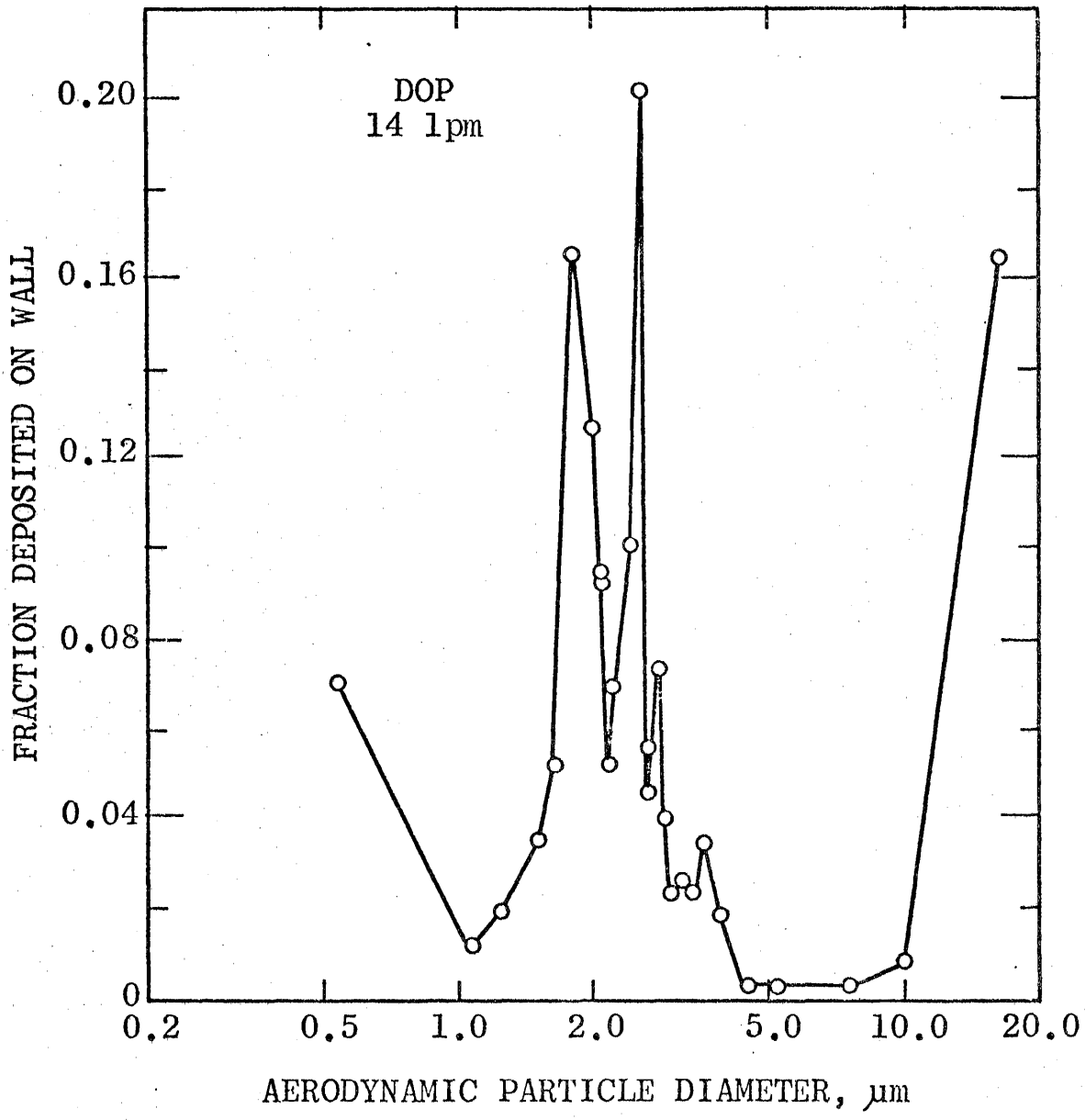

Figure 21

Total Wall Losses for DOP Particles

Table 4

STANDARD DEVIATIONS OF PARTICLE DEPOSITS
ON QUARTER SECTIONS OF THE FILTER

Aerodynamic Diameter, μm	Coarse Fraction Std. Dev., %	Fine Fraction Std. Dev., %
2.0	24	1
2.75*	7	8
3.5	2	14
7	9	154

*Particle size cut point.

5. Summary of dichotomous virtual impactor tests

The deposition curves were measured for monodisperse methylene blue particles at three different flow rates. The cut point at 14 ℓ/min. was found to be 2.8 μm rather than 3.5 μm as quoted by the manufacturer. The fine fraction filter deposit was significantly low for particles $\leq$ 1 μm diameter for flow rates greater than 10.7 ℓ/min. The DOP deposition curves showed fine structure which might be due to particle breakup. Total wall losses were less than 10% for the solid particles and less than 20% for the liquid particles, for particles less than 16 μm diameter. Near the cutoff, most of the particle loss was localized on the second stage. This loss could undoubtedly be reduced by improved design. The standard deviation of the deposits on quarter sections of the filters was less than 10% except for deposits on the filter containing less than 20% of the total mass.

On the basis of the above data, it is concluded that this dichotomous virtual impactor is a satisfactory sampler. It is recommended that the sampler be operated at 10.7 ℓ/min. where the cutoff is 3.2 μm and the sampling of the fine fraction has lower losses than at higher flow rates. The filter holders should be modified as discussed above. In use, the second stage should be examined and cleaned frequently to prevent clogging. An improvement in the design of the second stage would reduce the clogging problem and would probably also result in a smoother cutoff curve for liquid particles.

V. PRELIMINARY INVESTIGATION OF THE STACKED FILTER UNIT

The performance of the stacked filter unit has been examined in field trials[7,29] and limited laboratory measurements.[29] The available data are insufficient for a critical evaluation of the sampler. Uncertainty remains concerning the variation of the filtration characteristics with particle material, particle size, air flow rate, filter pore size and particle loading. One of the primary questions is the filtration efficiency of the large pore Nuclepore filter since there is a lack of pertinent experimental data and theoretical predictions.

Measurements of the filtration efficiency of 8 μm diameter pore size Nuclepore filters were made with monodisperse particles, using the techniques previously described. This work was carried out in collaboration with S. Goren and D. Plotkin, Department of Chemical Engineering, University of California, Berkeley. The results are presented in a paper prepared for publication which is reproduced in Appendix I.

The results obtained thus far indicate that particle bounce can lead to serious errors. The amount of bounce depends on the flow rate. The results also indicate that particles are sized primarily geometrically rather than aerodynamically. Additional work is needed to explore this effect further and more generally to obtain answers to the questions which were raised in the above discussion. Data are needed to provide a basis for the interpretation of sampling data, for the establishment of the limitations of the SFU and for optimization of the operating parameters.

VI. DEVELOPMENT OF A MANIFOLD FOR AMBIENT PARTICULATE SAMPLING

A. Manifold design

In anticipation of the need for parallel testing of several size-selective particulate samplers in ambient air, a manifold was designed and constructed with the following specifications:

1. The air intake is cylindrically symmetric for independence from wind direction.
2. The intake is 9 feet above the floor to avoid perturbations of air flow by nearby objects.
3. The manifold has a 50% cutoff of particles with an aerodynamic diameter of 20 μm.
4. Provision is made for 4 sampling lines, each sampling isokinetically from the manifold.

An assembly drawing of the manifold is shown in Figure 22. There are four lines which can be connected, for example, to the virtual dichotomous impactor, the AIHL cyclone, a total filter and an industrial hygiene cyclone. The manifold is pumped at 22.5 CFM by a hi-vol connected to the large pipe angling downward. The tripod is adjustable for flexibility in location. A framework is also provided for mounting wind speed and direction sensors at the top of the manifold. A detailed drawing of the manifold inlet is shown in Figure 23. Air enters the annular slit, then makes a 90 degree bend in an impaction stage designed for a 50% cutoff at 20 μm aerodynamic diameter. The impaction surface is sintered stainless steel saturated with oil to eliminate particle bounceoff. A feed system is provided to change the oil in the plate approximately once in 24 hours. This will allow almost indefinite operation without loading the plate. The use of sintered metal for an impaction surface is an innovation which was conceived and tested as a result of an investigation of particle

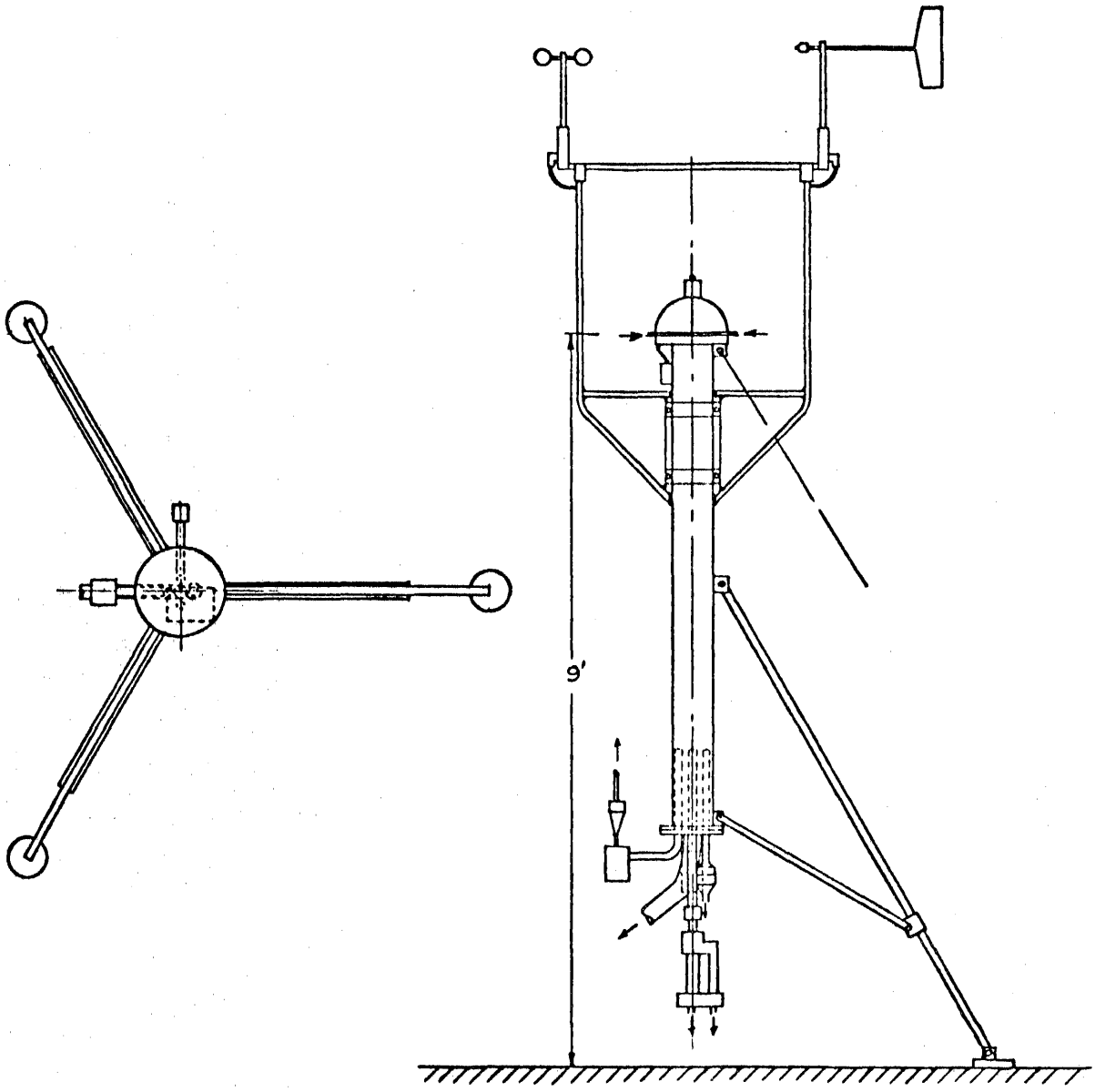

Figure 22 Assembly Drawing of the Sampling Manifold

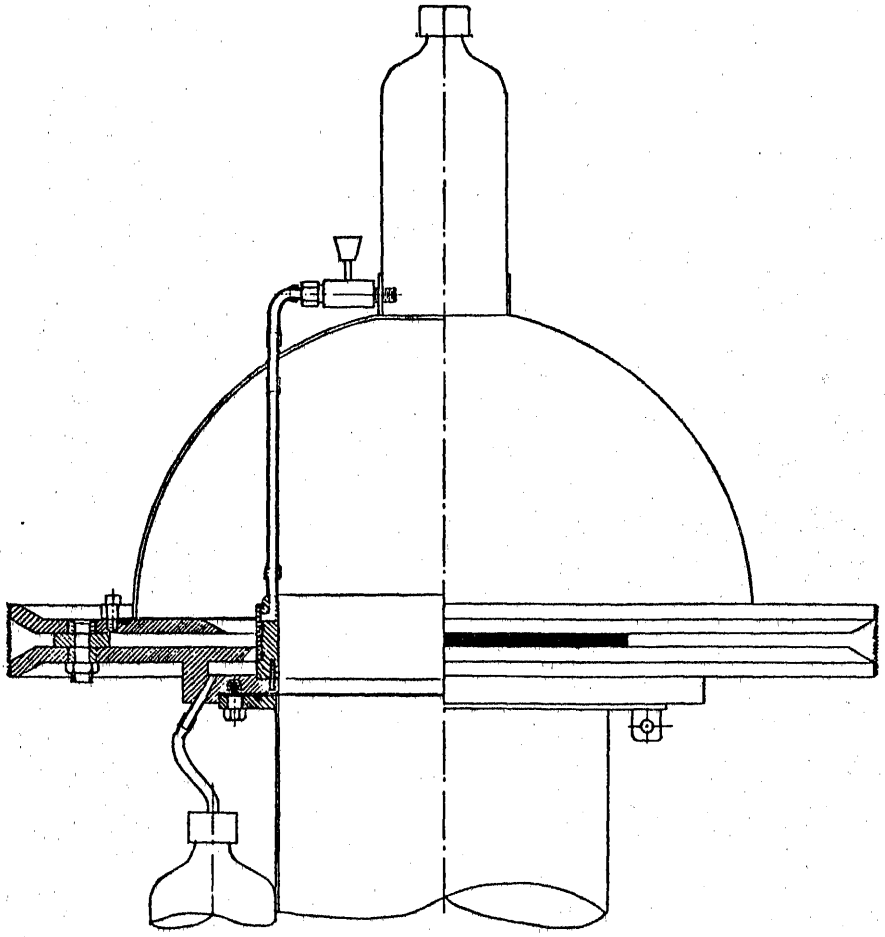

Figure 23
Manifold Inlet

bounce due to loading of impaction surfaces. This work is presented in Appendix II.

B. Wind run acquisition system

An electronics system was designed and constructed to accumulate the wind run with eight sector resolution. The system stores digital data which can be read out into a data logger. The Eight Sector Wind Run Acquisition System was designed to operate with a Met One Model 010 Anemometer and a Met One Model 020 Wind Direction Sensor. The instrument acquires pulses from the anemometer and counts them in one of eight sector counters according to the DC level supplied by the wind direction sensor. Sector one counts wind pulses from the 0^{o}-45^{o} (N-NE) direction, sector two 45^{o}-90^{o} (NW-N) direction (Note: these directions are relative to the orientation of the wind direction sensor). To keep the total number of counts per sector to three decades and to optimize resolution, an adjustable pre-scale (divider) feature is included. This number is set by a front panel thumbwheel switch which must be set greater than or equal to one.

Retrieval of data is accomplished by pulsing the Data Request line. This transfers data to output latches where it is held until the next data request. Once the output is latched, the counter and divider circuits are reset and resume counting. The latched, TTL compatible data may then be read in two hardwired selected manners:

1. All information may be read in parallel, this includes 3 BCD digits for each of the eight counters, 3 BCD digits of pre-scale information, 8 bits corresponding to eight overflow flags, and a master overflow indicating an overflow in any of the eight counters.

2. A second bussed mode involves putting data on a 12-bit bus as 10 words. These are 8 words of 3 BCD digits for the counters, a 3 BCD digits word for the pre-scaler, and an 8-bit overflow word. The master overflow bit exists but is not bus compatible. Selection of the specific word is made by the data requesting device.

VII. CONCLUSIONS AND DISCUSSION

A review of current techniques for size-selective sampling has revealed two instruments to be potentially suitable for monitoring purposes, namely the dichotomous virtual impactor and the cyclone. Both were subjected to extensive laboratory tests with well-characterized aerosol. Both were found to have satisfactory sampling characteristics and acceptable particle losses.

Each of the samplers has comparative advantages. The flow rate of the AIHL cyclone, 15 ℓ/min. is higher than the 10.7 ℓ/min. we recommend for the Sierra dichotomous. The cyclone could also be easily scaled up to higher flow rates whereas the dichotomous can be scaled above about 16 ℓ/min. only by adding additional jets, a cumbersome and expensive solution. The AIHL cyclone uses a larger filter (47 mm) compared to the dichotomous (37 mm), reducing the filter loading problem. The cyclone has no small orifices; the Sierra dichotomous may be prone to clogging on the second stage. The dichotomous has a major advantage in that it deposits the coarse fraction on a separate filter. In the case of the cyclone, the coarse fraction must be obtained by subtraction of the after-filter deposit from the total deposited on a separately run total filter, unless the deposit in the cyclone is extracted, a cumbersome process. The complete AIHL cyclone sampler is only slightly less expensive than the dichotomous, so that cost is not a basis for preference. The foregoing discussion is based on the results of laboratory tests. Laboratory tests, which determine the basic capabilities of the samplers, should be followed by field tests to investigate possible operational problems.

For the future, a sampler under development by Beckman Instruments for the U.S. Environmental Protection Agency[☆] promises to have important advantages. Current plans call for a fully automated dichotomous

[☆] R. Stevens, project officer

virtual impactor to be available January 1, 1979 at a mass production price. Automation eliminates the handling of individual samples with attendant operator errors and makes it feasible to change the filter whenever the pressure drop exceeds a predetermined value, thus improving the data collection during episodes.

The stacked filter unit does not satisfy the criteria for a monitoring instrument, the sampling rate being too low; however, its low cost makes the SFU an attractive candidate for special purpose sampling. The preliminary investigation has revealed that particle bounce is an important problem and that particles are sized primarily by geometrical rather than aerodynamic diameter. Additional work is needed to further explore these effects as well as to answer a number of remaining questions including the variation of the filtration characteristics with particle material, particle size, air flow rate, filter pore size and particle loading. These data are needed to establish the limitations of the SFU and for optimization of the operating parameters.

VIII. REFERENCES

1. Task Group on Lung Dynamics, "Deposition and Retention Models for Internal Dosimetry of the Human Respiratory Tract," Health Physics 12, 173-207 (1966).

2. H. L. Green and W. R. Lane, "Particulate Clouds: Dusts, Smokes and Mists", D. Van Nostrand Co., N.Y., 1957, Chap. 4.

3. K. Willeke, K. T. Whitby, W. E. Clark and V. A. Marple, "Size Distributions of Denver Aerosols - A Comparison of Two Sites," Atmos. Envir. 8, 609-633 (1974).

4. K. T. Whitby, W. E. Clark, V. A. Marple, G. M. Sverdrup, G. J. Sem, K. Willeke, B.Y.H. Liu and D.Y.H. Pui, "Characterization of California Aerosols--I. Size Distributions of Freeway Aerosol", Atmos. Envir. 9 463-482 (1975).

5. T. T. Mercer, Aerosol Technology in Hazard Evaluation, Academic Press, N.Y., 1973, pp 297-309.

6. T. G. Dzubay, R. K. Stevens and C. M. Peterson, "Application of the Dichotomous Sampler to the Characterization of Ambient Aerosols", in X-Ray Fluorescence Analysis of Environmental Samples, T. G. Dzubay, ed., Ann Arbor Science, Ann Arbor, Mich. (1977), pp. 95-105.

7. T. A. Cahill, L. L. Ashbaugh, J. B. Barone, R. A. Eldred, P. J. Feeney, R. G. Flocchini, C. Goodart, D. J. Shadoan and G. W. Wolfe, "Analysis of Respirable Fractions in Atmospheric Particulates via Sequential Filtration", J. Air Pollut. Control Assoc. 27, 675-678 (1977).

8. E. S. Macias, R. B. Husar and J. D. Husar, "Monitoring of Atmospheric Aerosol Mass and Sulfur Concentration", International Conference on Environmental Sensing and Assessment, Las Vegas, Nevada, Sept. 14-19, 1975.

9. John Baroni, et al., "Visibility Reduction: A Characterization of Three Urban Sites in California", Crocker Nuclear Laboratory, University of California, Davis, February 12, 1975 (submitted to Science).

10. G. M. Hidy, et al., "Characterization of Aerosols in California" (ACHEX), Finald Report, September 30, 1974 (revised April 1975), California Air Resources Board.

11. J. Samuels, S. Twiss and E. W. Wong, "Visibility, Light Scattering and Mass Concentration of Particulate Matter", Report of the California Tri-City Aerosol Sampling Project, July 1973, California Air Resources Board.

12. AIHA-Aerosol Technology Committee. "Guide for Respirable Mass Sampling". Amer. Ind. Hyg. Assoc. J. 31, 133 (1970).

13. J. J. Wesolowski, W. John, W. Devor, T. A. Cahill, P. J. Feeney, G. Wolfe and R. Flocchini, "Collection Surfaces of Cascade Impactors", in X-Ray Fluorescence Analysis of Environmental Samples, T. G. Dzubay, ed., Ann Arbor Science, Ann Arbor, Mich., 1977, pp 121-131.

14. A. K. Rao and K. T. Whitby, "Nonideal Collection Characteristics of Single Stage and Cascade Impactors", Am. Ind. Hyg. Assoc. J. 38, 174-179 (1977).

15. K. Miller and A. N. Manson, "Particulate Sizing Instrumentation and Regulation Development", Specialty Conference on Air Quality - Standards and Measurement sponsored by the Air Pollution Control Association, Kiamesha Lake, N.Y., October 13-15, 1974.

16. C. B. Shepherd and C. E. Lapple, "Flow Pattern and Pressure Drop in Cyclone Dust Collectors," Ind. Eng. Chem. 31, 972-984 (1939).

17. C. J. Stairmand, "The Design and Performance of Cyclone Separators", Trans. Instr. Chem. Engr. 29, 356-383 (1951).

18. W. B. Smith, K. M. Cushing, G. E. Lacey and J. D. McCain, "Particulate Sizing Techniques for Control Device Evaluation", Environmental Protection Agency Report EPA-650/2-74-102-a, available from the National Technical Information Service, Springfield, Virginia 22161, reference number PB 245 184.

19. H. C. Chang, "A Parallel Mutlicyclone Size-Selective Particulate Sampling Train", Amer. Ind. Hyg. Assoc. J. 35, 538-545 (1974).

20. M. W. Blachman and M. Lippmann, Amer. Ind. Hyg. Assoc. J. 35, 311-326 (1974).

21. H. E. Ayer and J. M. Hochstrasser, "Cyclone Discussion", University of Cincinnati, 1976 (unpublished paper).

22. D. Leith and D. Mehta, "Cyclone Performance and Design", Atmos. Environ. 7, 527-549 (1973).

23. R. N. Berglund and B.Y.H. Liu, "Generation of Monidisperse Aerosol Standards", Environ. Sci. and Technol. 7, 147-153 (1973).

24. D. M. Bernstein, M. T. Kleinman, T. J. Kneip, T. L. Chan and M. Lippmann, "A High-Volume Sampler for the Determination of Particle Size Distributions in Ambient Air", J. Air Poll. Control Assoc. 26, 1069-1072 (1976).

25. R. F. Hounam and R. J. Sherwood, "The Cascade Centripeter: A Device for Determining the Concentration and Size Distribution of Aerosols", Amer. Ind. Hyg. Assoc. J. 26, 122-131 (1965).

26. W. D. Conner, "An Inertial-Type Particle Separator for Collecting Large Samples", J. Air Poll. Control Assoc. 16, 35-38 (1966).

27. T. G. Dzubay and R. K. Stevens, "Ambient Air Analysis with Dichotomous Sampler and X-Ray Fluorescence Spectrometer", Environ. Sci and Technol. 9, 663-668 (1975).

28. B. W. Loo, J. M. Jaklevic and F.S. Goulding, "Dichotomous Virtual Impactors for Large Scale Monitoring of Airborne Particulate Matter", in Fine Particles, Aerosol Generation, Measurement, Sampling and Analysis, B.Y.H. Liu, ed., Academic Press, Inc., N.Y., 1976, pp 311-350.

29. R. D. Parker, G. H. Buzzard, T. G. Dzubay and J. P. Bell, "A Two-Stage Respirable Aerosol Sampler Using Nuclepore Filters in Series", Atmos. Environ. 11, 617-621 (1977).

IX. ACKNOWLEDGMENTS

We appreciate the interest and encouragement of J. Suder. G. Sasaki assisted with the laboratory tests. The field tests of the cyclone were supervised by B. Appel. We thank John Olin, Sierra Instruments, for the loan of the dichotomous sampler, and the Bay Area Air Pollution Control District for the use of their San Jose monitoring station. G. P. Reischl was partially supported by International Research Fellowship IF 05TW02271, National Institutes of Health.

APPENDIX I

ANOMALOUS FILTRATION OF SOLID PARTICLES BY NUCLEPORE FILTERS**

W. John* and G. Reischl
Air and Industrial Hygiene Laboratory
California Department of Health, Berkeley, CA 94704, U.S.A.

S. Goren and D. Plotkin
Department of Chemical Engineering
University of California, Berkeley, CA 94720, U.S.A.

ABSTRACT

Because of recent interest in the use of stacked Nuclepore filters as a particle size-selective sampler, the filtration efficiency of 8 μm pore size Nuclepore filters has been measured for laboratory aerosols. Lower efficiencies are obtained for solid particles than for liquid particles, probably due to particle bounce. Interception appears to be the dominant filtration mechanism.

INTRODUCTION

The use of a sequence of Nuclepore filters as a particle size-selective sampler was suggested by Spurny, et al. (1969 b) and studied by Melo and Phillips (1974). Recently, a two-filter sampler for the separation of respirable and non-respirable particles in ambient air has been investigated by Parker, et al. (1977) and Cahill, et al. (1977). This attractively simple device produces samples suitable for X ray fluorescence analysis. In attempting to validate the sequential filtration sampler, we have measured the filtration efficiency for laboratory aerosols.

MEASUREMENTS

We have investigated the sequential filtration unit used by Cahill, et al. (1977), consisting of an 8 μm pore size Nuclepore filter followed by a 0.4 μm pore size filter, both held in a double 47 mm filter holder***. Monodisperse, neutralized aerosols were produced by a Berglund-Liu vibrating orifice generator. The aerosols included viscous liquid particles, 75% v/v glycerol, 25% v/v uranine, and solid, spherical particles of methylene blue. The loaded filters were sonicated in alcohol-water solution; uranine was quantitated on a fluorimeter and methylene blue on a spectrophotometer. The efficiency of the 8 μm filter was determined by dividing the deposit on that filter by the sum of the deposits on both filters and the supporting grid for the 8 μm filter. The deposit on the plastic supporting grid, obtained by washing it with solvent, was approximately 10% of the total, depending on particle size. The filter loadings were kept relatively light to avoid loading problems.

**Work partially supported by the California Air Resources Board.
***Nuclepore Corp., Pleasanton, CA, U.S.A.

RESULTS AND DISCUSSION

Figure 1 shows that the collection efficiencies of the 8 μm Nuclepore filter for methylene blue and glycerol-uranine particles agree for small particle size but the efficiency for methylene blue falls significantly below that for glycerol-uranine with increasing particle size. Finally, both efficiencies approach 100% as the particle diameter approaches the pore diameter. Figure 2 shows that the methylene blue efficiencies agree better with the glycerol-uranine efficiencies when the face velocity is reduced from 6 cm/sec to 2.4 cm/sec.

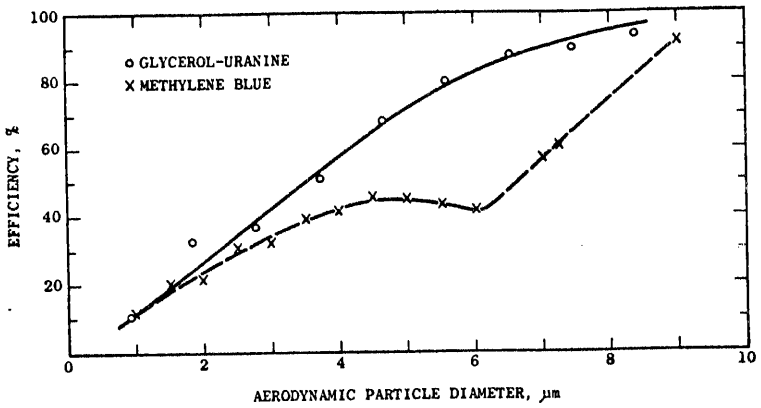

Figure 1. Measured filtration efficiency of 8 μm pore size Nuclepore filters for methylene blue particles compared to that for glycerol-uranine particles. The flow rate was 5 ℓpm (face velocity 6 cm/sec, based on an exposed area 42 mm in dia.)

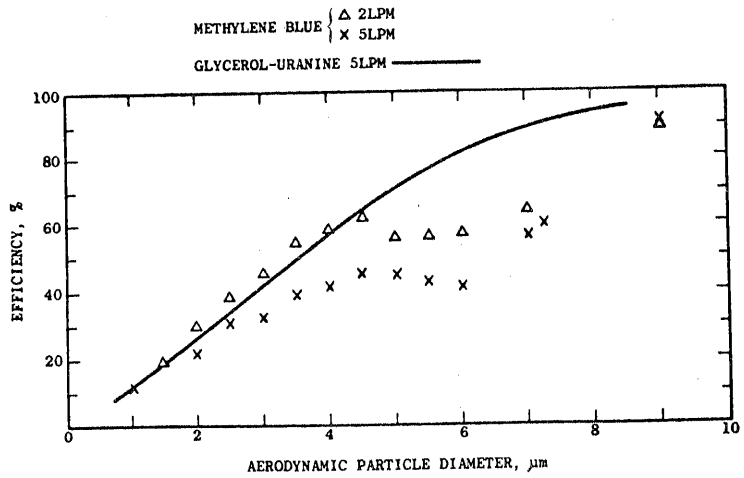

Figure 2. Filtration efficiency for methylene blue particles taken at two flow rates, 2 ℓpm (triangles) and 5 ℓpm (crosses). The line representing the glycerol-uranine data is repeated from Figure 1.

The lower efficiency for methylene blue may be explained by particle bounce. The observed increase of efficiency with decreasing face velocity is consistent with this hypothesis. Microscopic examination showed that the glycerol-uranine particles were deposited mostly on the periphery of the pores. Thus, after bouncing, the methylene blue particles would have a high probability of penetrating the filter. The possibility of particle bounce was discussed by Parker, et al. (1977). Some evidence of particle bounce, although inconclusive, was obtained by Parker and Buzzard (1977). Earlier, Spurny and Madelaine (1971) suggested that particle bounce might explain their observation of lowered efficiency for 0.357 μm latex particles at high flow rates.

The glycerol-uranine efficiencies are well-fitted by a calculation using interception alone. For uniform flow, we calculate the efficiency for interception to be:

$$(1)\quad \varepsilon = 2R - R^2$$

where R is a dimensionless parameter defined as the ratio of the particle diameter to the pore diameter. Equation (1), shown as the dashed line in Figure 3, somewhat overestimates the filtration efficiency, although it is surprisingly close considering the simplicity of the calculation. A better fit is obtained by using a more realistic non-uniform flow from Happel and Brenner (1973) who calculated creeping flow through an orifice using oblate spheroidal coordinates. From the stream function, we obtain for the interception efficiency:

$$(2)\quad \varepsilon = (2R - R^2)^{3/2}$$

Shown as the solid line in Figure 3, Equation (2) is a very good fit to the glycerol-uranine points. The more realistic flow near the hole edge improves the fit for small particles which must pass near the hole edge to be intercepted. This may explain the overestimation of interception obtained by Spurny, et al. (1969 a) who used a uniform flow calculation. The apparent absence of impaction in the present experiment may be explained qualitatively from a consideration of the streamlines. As a particle approaches the filter from a distance, it follows streamlines which curve toward the pore. In the region near the pore, the streamlines curve in the opposite direction. This tends to cancel drift across streamlines caused by inertia, an effect discussed by Smith and Phillips (1975). We suppose that the cancellation is fortuitously nearly complete for the present experimental parameters. Additional experiments are necessary to confirm the absence of impaction and to determine its possible importance at higher flow rates.

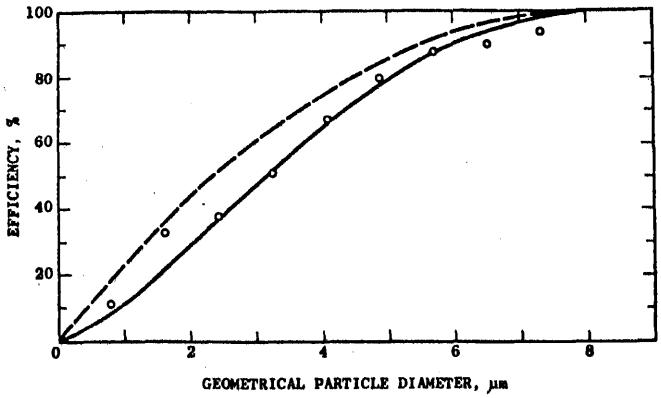

Figure 3.. Comparison of measured efficiency for glycerol-uranine particles (data points) and theoretical calculations of interception. Geometrical particle diameter, the appropriate variable for interception, is used as the abscissa. The dashed line is calculated for uniform flow (Equation 1), the solid line for non-uniform flow (Equation 2) through an orifice.

CONCLUSIONS

The present work demonstrates that particle bounce is an important phenomenon in filtration by large pore size Nuclepore filters and that interception is apparently the dominant filtration mechanism. For the use of sequential filters in atmospheric sampling, these results imply that the particles are sized geometrically rather than aerodynamically. Particle bounce could lead to serious errors. In a more general sense, the present results show that additional work is necessary in order to improve understanding of the filtration process with Nuclepore filters. We are currently extending our investigation.

REFERENCES

Cahill T.A., Ashbaugh L.L., Barone J.B., Eldred R.A., Feeney P.J., Flocchini R.G., Goodart C., Shadoan D.J. and Wolfe G.W. (1977) Analysis of Respirable Fractions in Atmospheric Particulates via Sequential Filtration. J. Air Pollut. Control Assn. 27, 675-678.

Happel J. and Brenner H. (1973) Low Reynolds Number Hydrodynamics, second revised edition, pp 150-153. Noordhoff International Publishing, Leyden, The Netherlands.

Melo O.T. and Phillips C.R.(1974) Aerosol-Size Spectra by Means of Membrane Filters. Environ. Sci. Technol. 8, 67-71.

Parker R.D. and Buzzard G.H. (1977) A Filtration Model for Large Pore Nuclepore Filters. (Unpublished)

Parker R.D., Buzzard G.H., Dzubay T.G. and Bell J.P. (1977) A Two Stage Respirable Aerosol Sampler Using Nuclepore Filters in Series. Atmospheric Environment 11. 617-621.

Smith T.N. and Phillips C.R. (1975) Inertial Collection of Aerosol Particles at Circular Aperture. Environ. Sci. Technol. 9, 564-568.

Spurny K.R., Lodge J.P., Jr., Frank E.R. and Sheesley D.C. (1969 a) Aerosol Filtration by Means of Nuclepore Filters: Structural and Filtration Properties. Environ. Sci. Technol. 3, 453-464.

Spurny K.R., Lodge J.P., Jr., Frank E.R. and Sheesley D.C. (1969 b) Aerosol Filtration by Means of Nuclepore Filters: Aerosol Sampling and Measurement. Environ. Sci. Technol. 3, 464-468.

Spurny K. and Madelaine G. (1971) Efficiency Measurement of Nuclear Pore Filters by Means of Latex Aerosols. Collection Czechoslov. Chem. Commun. 36, 2857-2866.

APPENDIX II

THE COLLECTION EFFICIENCY OF IMPACTION SURFACES: A NEW IMPACTION SURFACE

Abstract

One of the major drawbacks to the use of cascade impactors is particle bounceoff. Coating the surface with a sticky substance does not eliminate the problem, since as the deposit accumulates, particles will bounce off previously deposited particles which are not submerged in the coating substance. This results in decreasing collection efficiency of the impaction stage and an erroneous result due to deposition of reentrained particles on subsequent stages. A theory has been developed to account quantitatively for the loading effect. Measurements with monodisperse aerosol were found to be in excellent agreement with the theory.

A new impaction surface has been developed which consists of a sintered stainless steel plate saturated with a low viscosity oil. The oil coats the surface of the plate and the deposited particles by capillary action while the porous metal prevents blowoff of the oil. This surface has essentially 100% sticking efficiency, independent of loading.

Table of nomenclature:

F ..... Flow rate ($l \cdot min^{-1}$)

C_N ..... Aerosol concentration (l^{-1})

C_M ..... Mass concentration of aerosol ($mg \cdot m^{-3}$)

d ..... Geometric particle diameter (μm)

ρ ..... Density of the particles ($g \cdot cm^{-3}$)

A ..... Total impaction area (cm^2)

Y ..... Particle effective area coefficient, dimensionless

f_o ..... Probability that a particle impacts on the stage

f_1 ..... Sticking probability for a particle impacting on the portion of the surface free of deposited particles

f_2 ..... Sticking probability for a particle impacting on already deposited particles*

α ..... Ratio of the effective area of a particle to the total area, dimensionless

β ..... Number of particles striking the impaction area per unit time (s^{-1})

a ..... Fractional area flux per unit time (s^{-1})

b ..... Fraction of area covered at time t

N ..... Cumulative number of particles which have been deposited on the impaction plate at time t

N_T ..... Cumulative number of particles which have been sampled at time t

δE ..... Instantaneous collection efficiency

E ..... Integrated collection efficiency

M ..... Total mass sampled (mg)

*This does not imply that a particle has to be deposited where it impacts for the first time. It can also bounce off and then be deposited elsewhere on the plate, e.g., in a halo around the primary impaction area.

It is well known that one of the major drawbacks to the use of cascade impactors is particle bounce-off, i.e., the failure of particles to stick to the impaction surface. For this reason, it is customary to coat the surface with a sticky substance such as vacuum grease. Even this does not eliminate the problem since, as the deposit accumulates, particles will begin to bounce off previously deposited particles. The particles are not coated by the greases normally used since the viscosity must be high enough to prevent flow away from the jet. The following theory is designed to account for the loading effect quantitatively.

When a particle is incident on an impaction surface already partially covered with particles, the probability that the particle will strike a clear area of the surface is just proportional to the fraction of the surface which is clear of particles, assuming that the particle is incident randomly. Thus, the rate of change of b, the fraction of area covered at time t, is given by:

$$(1)\quad \frac{d\,b(t)}{dt} = f_1\, a[1-b(t)]$$

where f_1 is the sticking probability for the particle-free surface. The constant a is the fractional area flux per unit time. a is given by:

$$a = \alpha \cdot \beta$$

where $\alpha = \frac{\gamma \pi d^2}{4A} \cdot 10^{-8}$ is the ratio of the effective area of a particle to the total area. γ is a coefficient which accounts for the fact that the effective area occupied by a particle is different from the cross sectional area of a particle. γ depends on the particle shape and the geometrical arrangement (packing) of the particles on the surface.

β, the number of particles striking the impaction area per unit time, may be written:

$$\beta = \frac{F\, C_N\, f_o}{60} = \frac{F\, C_M\, f_o}{\pi d^3 \rho} \cdot 10^5$$

Equation (1) may be integrated to yield:

$$(2) \quad b(t) = 1 - e^{-f_1 at}$$

The integration constant was taken from the initial condition $b(o) = o$.

The rate of change of the number of particles deposited is given by the following equation:

$$(3) \quad \frac{dN(t)}{dt} = \beta[(1-b)f_1 + b\, f_2]$$

The first term is the rate of deposition from impaction on clear surface, the second from impaction on particles.

Also, the rate of change of the total number of particles sampled is:

$$(4) \quad \frac{dN_T}{dt} = \frac{\beta}{f_o}$$

Then the instantaneous collection efficiency can be derived:

$$(5) \quad \delta E(t) = \frac{dN}{dt} \Big/ \frac{dN_T}{dt} = f_o\, [(f_1 - f_2)e^{-f_1 at} + f_2]$$

The integrated collection efficiency is derived by integrating equation (3) to obtain N, integrating equation (4) to obtain N_T, and dividing. The result is:

$$(6) \quad E(t) = \frac{N}{N_T} = f_o\, [(f_1 - f_2)\, (\frac{1 - e^{-f_1 at}}{f_1 at}) + f_2\,]$$

The limiting values of δE and E are the same:

$$t = o, \ \delta E = E = f_o\, f_1$$

$$t \rightarrow \infty; \ \delta E, \quad E \rightarrow f_o\, f_2$$

The collection efficiencies are given as a function of time by equations (5) and (6). Normally, an impactor is operated over a period of time, beginning with a clean surface. Then the integrated collection efficiency E is appropriate where t is the total exposure time. The instantaneous collection efficiency, δE is useful if, for example, an impaction stage is followed by a particle counter.

Equations (5) and (6) can also be written in terms of the total mass sampled (total mass entering the sampler whether or not it is deposited).

$$(7) \quad \delta E(M) = f_o[(f_1-f_2)e^{-kM} + f_2]$$

$$(8) \quad E(M) = f_o[(f_1-f_2)\left(\frac{1-e^{-kM}}{kM}\right) + f_2]$$

where

$$(9) \quad k = \frac{15Y\, f_o f_1}{A\, d\, \rho}$$

Experimental Verification of the Theory

Experimental Methods:

The theory was tested by comparing Eq. (7) and Eq. (8) to measurements of the deposition of particles on a grease-coated impaction surface. Complications were encountered from the non-ideal performance of the impactor used, the Delron CS-6. When operated at the normal flow rate, the deposit on stage 1 is not uniform in density. A ring of secondary deposits from bounce-off or reentrainment forms outside of the central spot. In order to remove the secondary ring from the impaction plate, the impactor was operated at a higher than normal flow rate. In addition, two different stage configurations were employed for these measurements, designated

Impactor A and Impactor B. Impactor A, shown in Figure 1, involves the use of stage 2 without an impaction plate as a prefocuser for the aerosol which then enters impaction stage 1. For operation at 25 lpm, the 50% cutpoint is 12.4 μm. Impactor B, shown in Figure 2, reverses the order of the stages. The 50% cutpoint for Impactor B is 5.7 μm at 25 lpm.

The experimental setup for the initial measurements is shown in Figure 3. Monodisperse particles were made by a Berglund-Liu vibrating orifice aerosol generator. Bounce-off effects depend on particle size; since one of the main applications of the present study is to ambient air measurements, an aerodynamic particle diameter of 20 μm was chosen for use. Because of this relatively large particle size, the aerosol generator was operated upside down with the subsequent aerosol conditioning devices arranged in a vertical straight line to reduce impaction and sedimentation losses. An offset had to be introduced just before the impactor to prevent agglomerates from falling into the impactor. The impactor was pumped by a Sierra Instruments automatic flow controller. Aerosol size and concentration was continuously monitored with a Climet 201 optical counter.

Impaction Stage Efficiency:

The probability that a particle impacts on the stage, f_o, was evaluated by measuring the deposition of liquid particles which have essentially zero bounce-off probability. 20 μm DOP (Di-n-octalphthalate) particles were used with disodium fluorescein added. The fluorescein, being insoluble in DOP, formed a 2 μm diameter core in the particle. A Nuclepore afterfilter with 0.8 μm pores was used to ensure retention of the fluorescein cores.

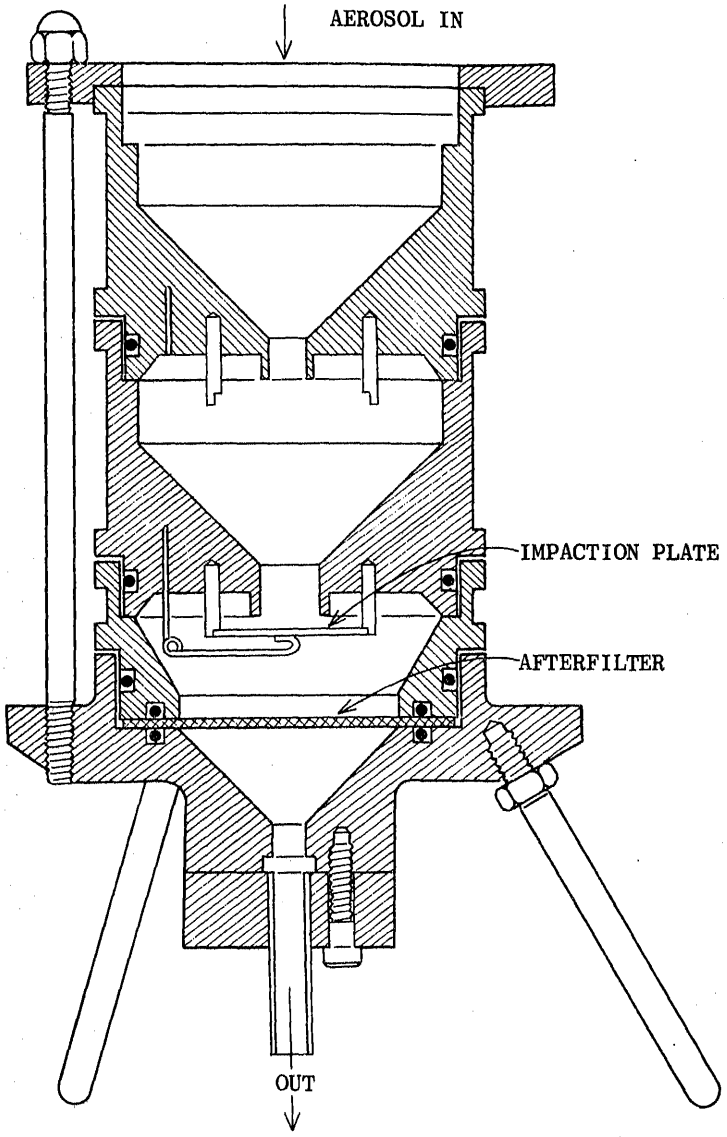

Figure 1

Impactor A Used in the Measurements

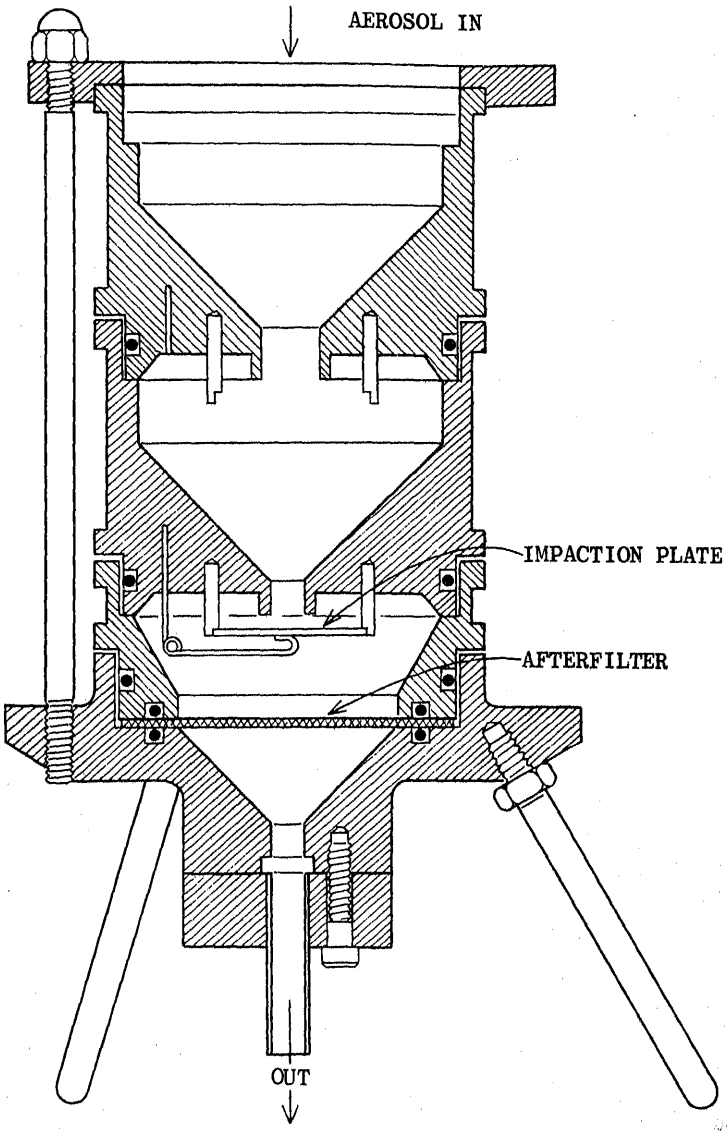

Figure 2

Impactor B

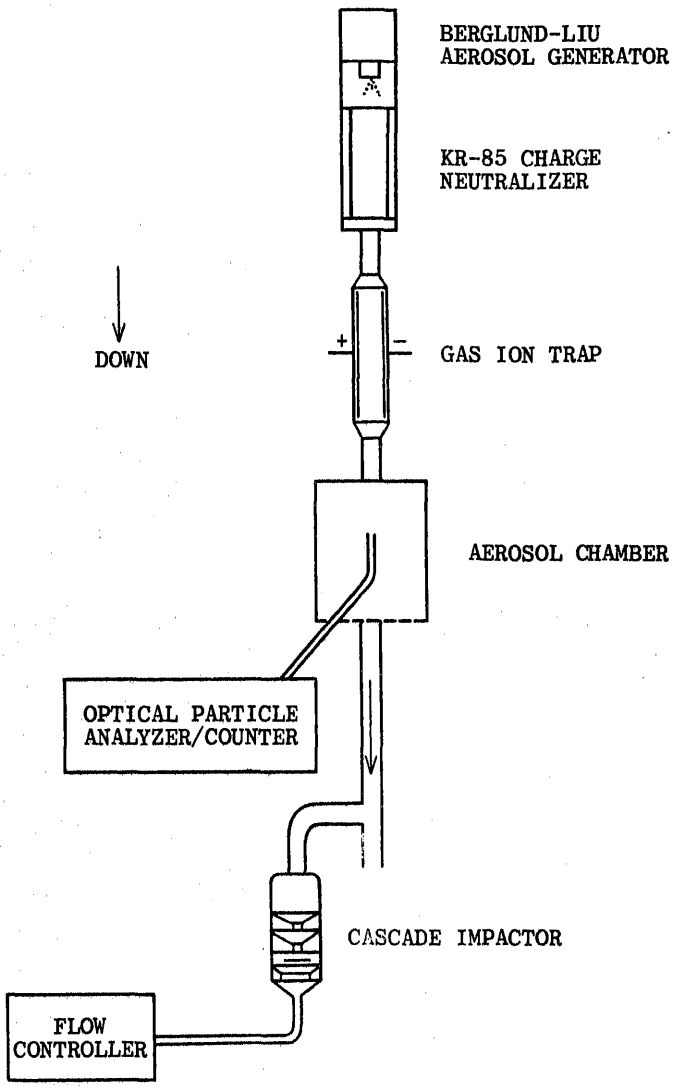

Figure 3

Experimental Arrangement for the Measurement of Integrated Deposition Efficiency

The deposits on the stainless steel impaction plate, the walls surrounding the impaction stage and the afterfilter were separately dissolved in an 85% isopropyl alcohol-15% water solution and quantitated on a Turner fluorometer. Three measurements made at different mass loadings were in good agreement, showing that there was no loading effect or blow-off of the DOP. The stage efficiency f_o was found to be 0.80 ± 0.04 for Impactor A and 0.96 ± 0.02 for Impactor B.

Integral Deposition Efficiency

For the study of bounce-off, it is desirable to use solid, highly elastic particles. It was found that potassium biphthalate ($KHC_8H_4O_4$) particles are quite suitable. Observed under a microscope, they appear to be extremely smooth spheres. The particles were generated with a 15.6 μm geometric diameter (20 μm aerodynamic diameter) and a relative standard deviation better than 4.5%. Disodium fluorescein was added as a tracer.

Each data point involved sampling the aerosol with Impactor A for a certain time period, beginning with a fresh silicone* grease-coated surface. Then the deposits on the plate, walls and afterfilter were dissolved in 50-50 isopropyl alcohol-water solution for quantitation. It was found that potassium biphthalate quenches the fluorescence of disodium fluorescein, necessitating a calibration of the fluorometer. The integrated efficiency E was obtained by dividing the mass on the plate by the sum of the masses on the plate, walls and afterfilter.

*Dow-Corning

Comparison to the Theory:

The data are shown in Figure 4. The observed deposition efficiency falls off rapidly at first and then more slowly. The line through the data is calculated from Equation (8) with the parameters determined as follows:

(a) f_o is taken from the DOP measurement of the stage efficiency.

(b) f_1 is found from the extrapolation to M = 0. The result is $f_1 = 1$, indicating that all the particles stick to the fresh silicone surface.

(c) f_2 was found to be 0.2 by fitting the data at large M.

(d) k was evaluated by fitting Equation 8 to the point corresponding to E = 50%.

The above fitting procedure used three data points. It can be seen from Figure 4 that the curve fits the data very well over the entire range.

Microscopy of the Deposits:

From the value of k and Eq. (9), it is possible to obtain the value of the particle effective area coefficient γ, but the area A must first be determined. This was done by measuring the density profile of a deposit under the microscope. The silicone-coated plate was loaded with about 4 mg of material for this purpose. The deposit profiles of Impactor A and Impactor B are shown in Figure 5 and Figure 6, respectively. The profile for Impactor A is Gaussian in appearance, with a half-width nearly equal to the diameter of the orifice. The profile for Impactor B is fairly flat on top, but the half-width is less than the orifice diameter. The particles in the wings of the distributions include secondary deposits of particles which bounced

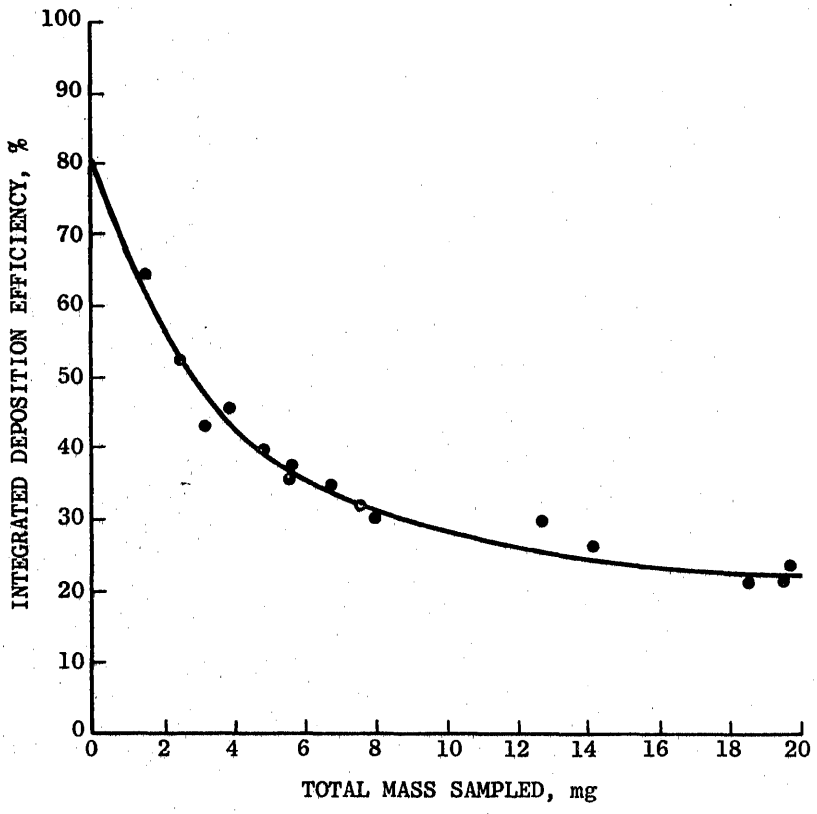

Figure 4

Integrated Deposition Efficiency for Potassium Biphthalate Particles on the Silicone Grease-Coated Impaction Stage of Impactor A. The Line is Equation 8 Fitted to the Data.

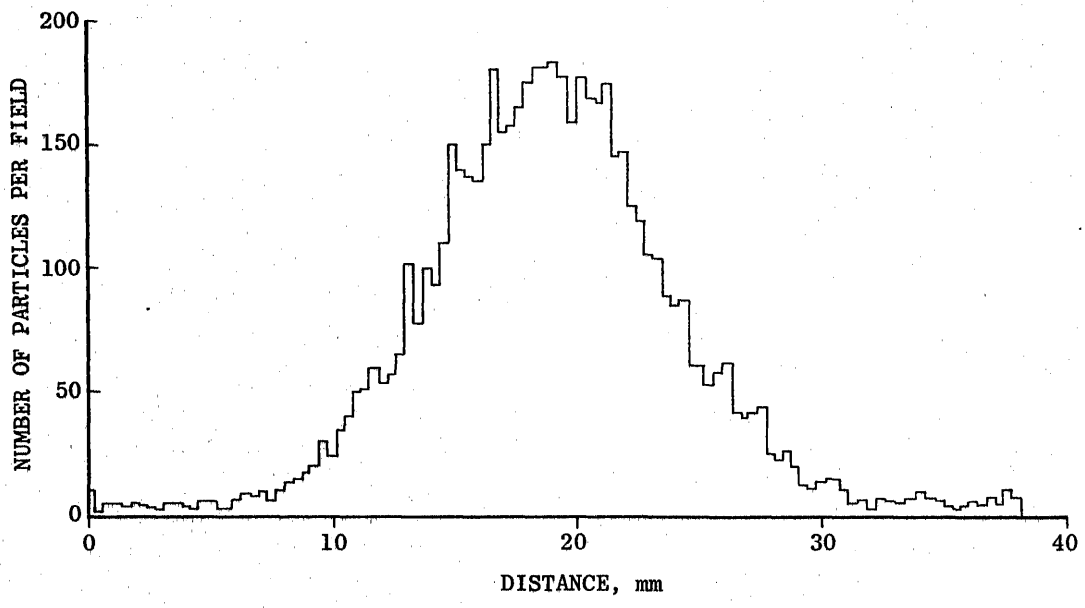

Figure 5

Profile of Particle Deposit on the Stage of Impactor A

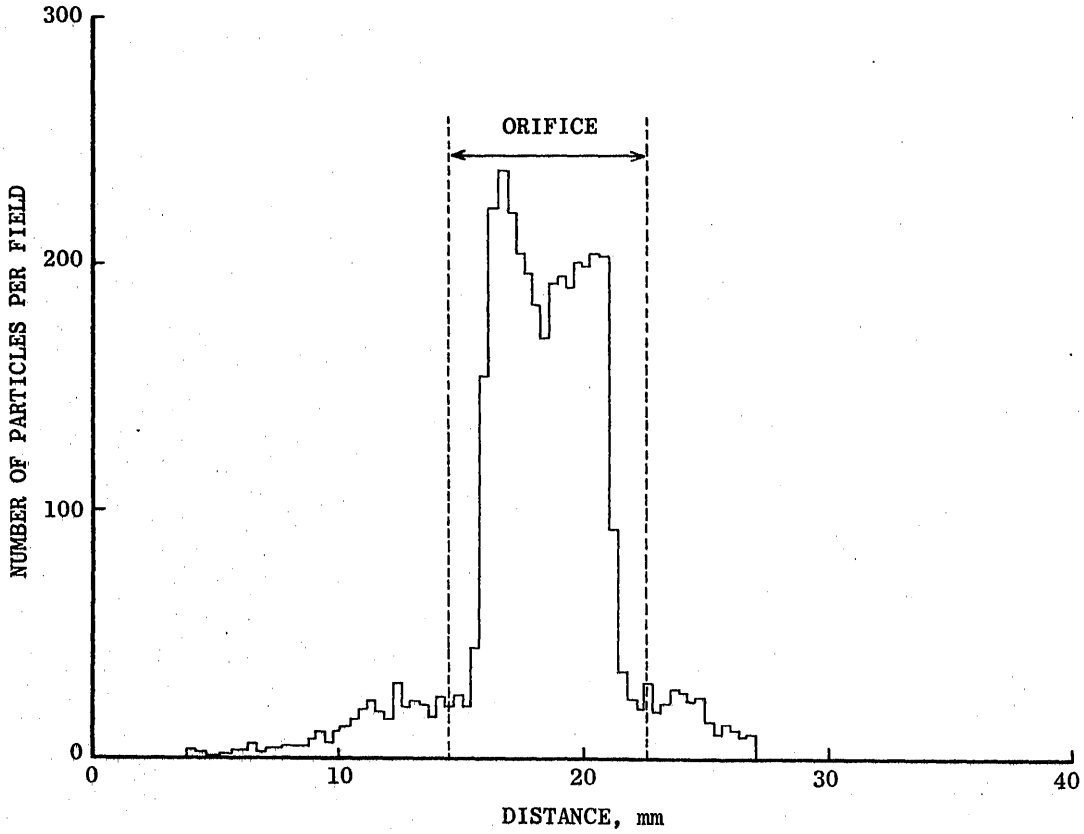

Figure 6

Profile of the Particle Deposit on the Stage of Impactor B

from the primary impaction spot. This makes the determination of the primary area uncertain. We have arbitrarily taken the diameter of the primary area to be the mean between the half-width of the deposit profile and the orifice diameter. The result for the primary impaction area is $A = 1.13$ cm^2 for Impactor A and 0.385 cm^2 for Impactor B.

Under the microscope, the particles in the central spot were seen not to be packed in a hexagonal array corresponding to closest packing but more like a square array. No particles were seen deposited on other particles, indicating that particles impacting on already deposited particles bounced off. From the area A and the measured integral efficiency, we obtain $\gamma = 1.27$. This value is identical with the fractional area covered by spheres in a square packing array. However, this must be somewhat fortuitous in that the effective area for the impaction of two spheres is larger than the projected area of one sphere. We suppose that the recoil of the struck spheres causes them to pack somewhat more tightly. Because the process is complicated, it is not profitable to pursue the interpretation of γ further at this time.

Instantaneous Collection Efficiency:

The experimental arrangement shown in Figure 7 was used to measure δE. The apparatus upstream of the aerosol chamber was the same as in Figure 3. The particles which were not deposited in the impactor were counted in real time by the Climet optical particle analyzer and an Ortec pulse counter-timer. A Sinclair aerosol photometer was used to monitor the aerosol concentration from the chamber. The aerosol sampling rate was first measured

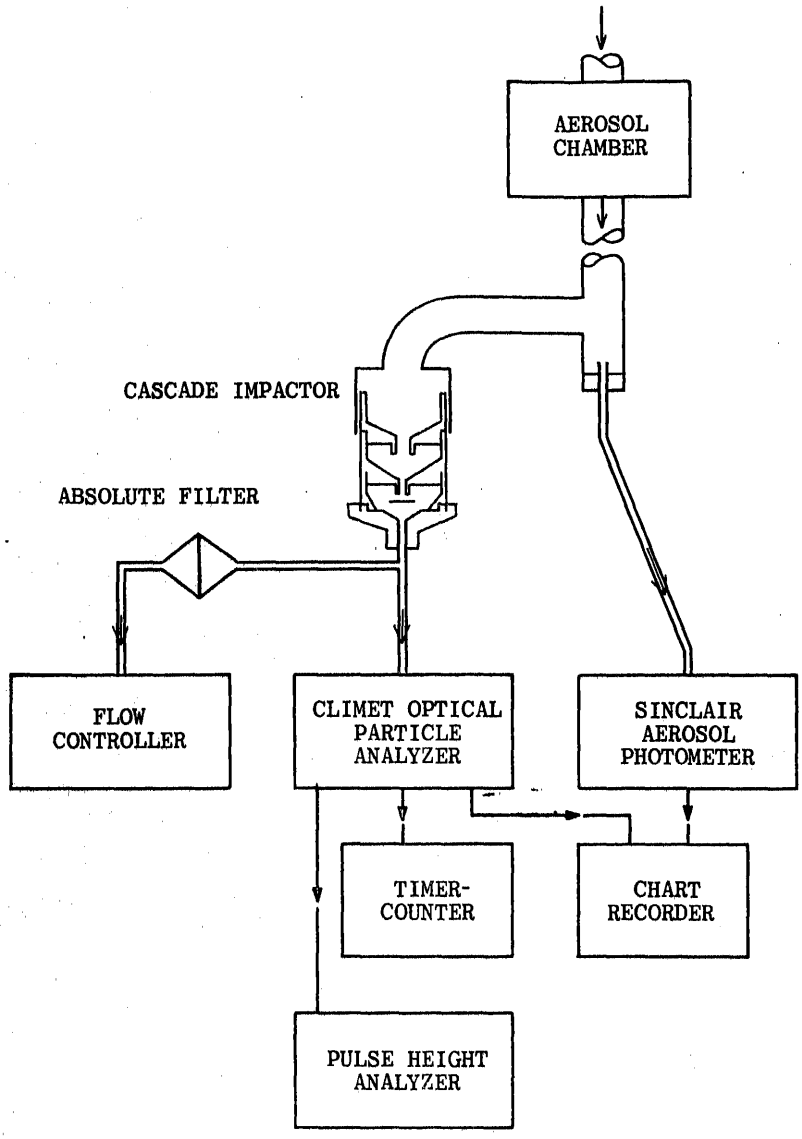

Figure 7

Experimental Arrangement for the Measurement of the Instantaneous Deposition Efficiency

by taking the Climet count with the impactor plate removed. The impactor plate was then replaced for the measurements. The Sinclair aerosol photometer output signal, which is dependent on particle size and concentration, was used to verify that those parameters were constant throughout the measurements.

It was also necessary to take into account the deposition of particles on the walls. The data reported above on the integral efficiency included direct measurements of the wall deposit by chemistry. The percentage lost to the walls [wall/(afterfilter + wall)] was 57.4 $\pm$ 4.5% for loads from 1 to 20 mg. Thus, to a good approximation, the fraction lost to the walls was independent of load, a reasonable result since most of the loss was below the impaction zone on the tapered wall leading to the afterfilter. The wall loss was, therefore, evaluated from the previous data. The results obtained with Impactor A are shown in Figure 8. $\delta E/f_o$ has been plotted, which is the sticking efficiency since the stage efficiency f_o has been divided out. The line is calculated from the theory using the same values for the parameters as for the fit to the integral efficiency data (Figure 4). It can be seen that the fit is very good.

Figure 9 shows the results obtained with Impactor B. Impactor B loads considerably faster than Impactor A because of the smaller impaction area. The theoretical line uses the measured stage efficiency $f_o = 0.96$ and the values $f_1 = 1$, $f_2 = 0$ and $\gamma = 1.27$. The zero value for f_2 is remarkable in that it implies that the potassium biphthalate particles do not stick at all to previously deposited particles, as was inferred from the microscope

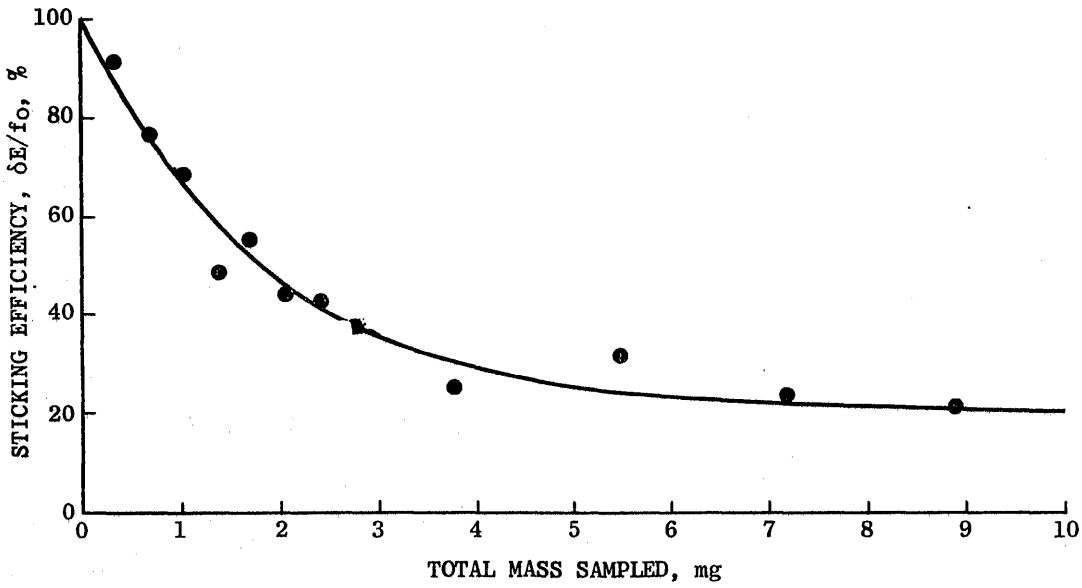

Figure 8

Measured Instantaneous Sticking Efficiency vs. Total Mass Sampled with Impactor A. The Line is a Fit of Equation 7 to the Data.

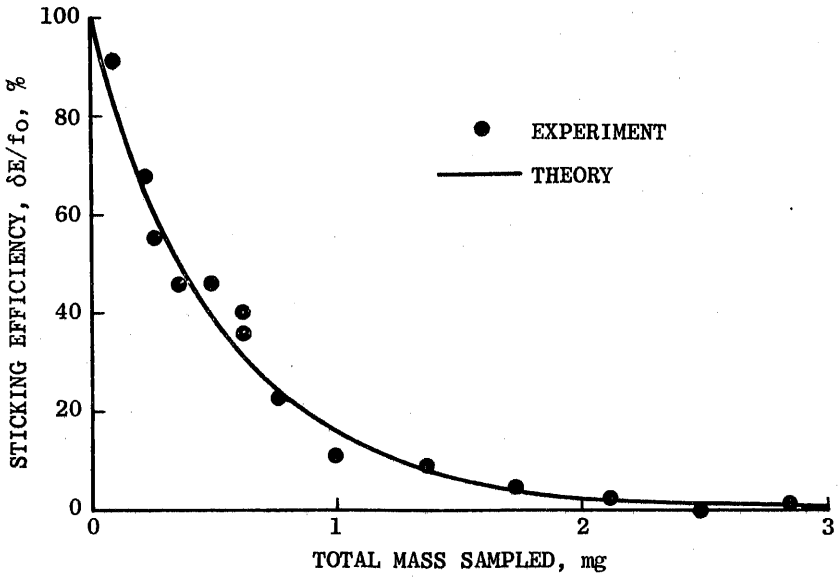

Figure 9

Measured Instantaneous Sticking Efficiency vs. Total Mass Sampled with Impactor B. The Line is a Fit of Equation 7 to the Data.

examination. Therefore, the non-zero value for f_2 (0.2) obtained for Impactor A is to be interpreted as representing the secondary deposition of bounce-off particles. The secondary area loads much more slowly and, therefore, remains sticky even for high total sample.

Discussion of the Loading of Impaction Surfaces:

The results above show that the theory represented by Eq. (7) and Eq. (8) accounts quantitatively for the measurements of the instantaneous and integral efficiencies. It is useful to replot the integral sticking efficiency against the calculated density of the load on the plate. This has been done in Figure 10 for Impactor A using two different values of the parameter f_2, the value $f_2 = 0.2$ which fits the data for Impactor A and a hypothetical value $f_2 = 0$. For $f_2 = 0$, the efficiency goes to zero at 1.33 mg/cm^2 corresponding to a monolayer on the surface (this includes the value 1.27 for γ, the effective particle area coefficient). In Figure 11, the sticking efficiency is plotted vs. load density for Impactor B where the fit required $f_2 = 0$.

These results, particularly as displayed in Figure 10, emphasize the fact that loads greater than a monolayer can only be obtained as a result of particles sticking to particles or particles being deposited in a secondary zone after bouncing from the primary impaction spot. The latter probability depends on the design of the impactor in question. Further, Figure 10 can be used to assess the error corresponding to a given plate load. If, for example, a 20% error is acceptable, a load density of about half a monolayer can be accumulated. Although a monolayer is a useful parameter to gauge the load density, it is well to bear in mind that a monolayer can be achieved only asymptotically since the deposition is assumed to be a random process (see Eq. 2).

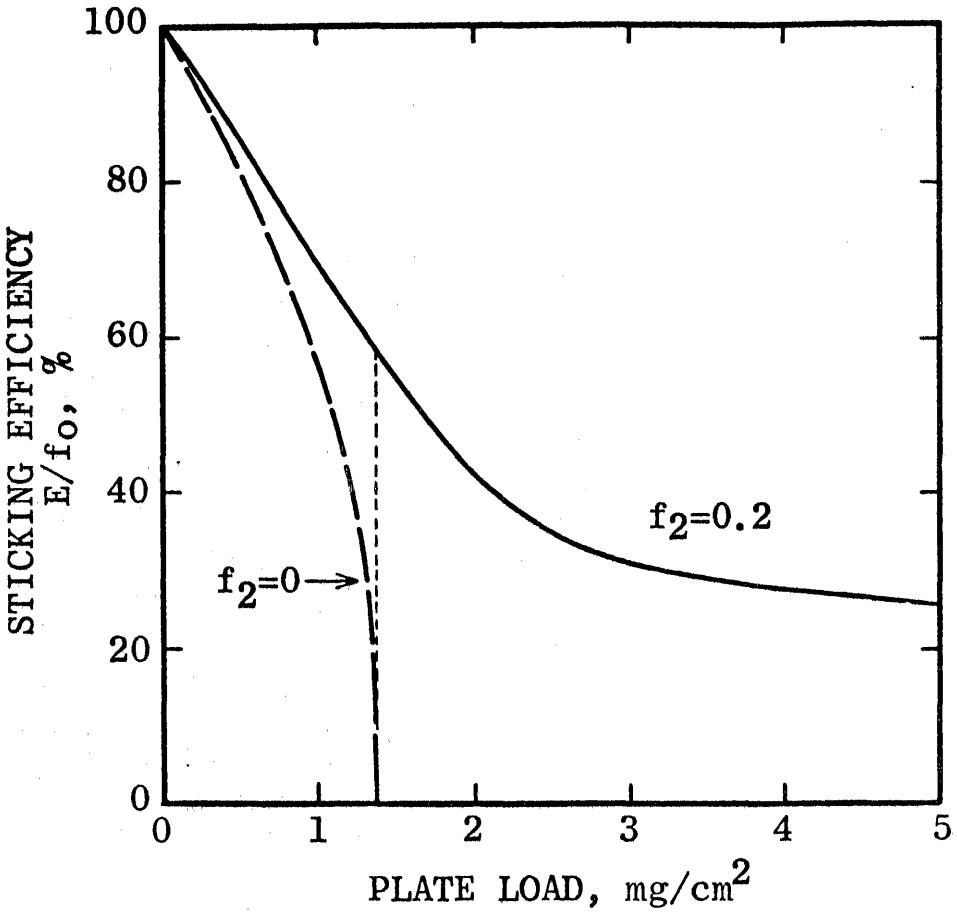

Figure 10

Integrated sticking efficiency vs. plate deposit density calculated for Impactor A from Equation 8 for two values of the parameter f_2. The vertical line at 1.3 mg/cm^2 corresponds to a monolayer of particles on the surface.

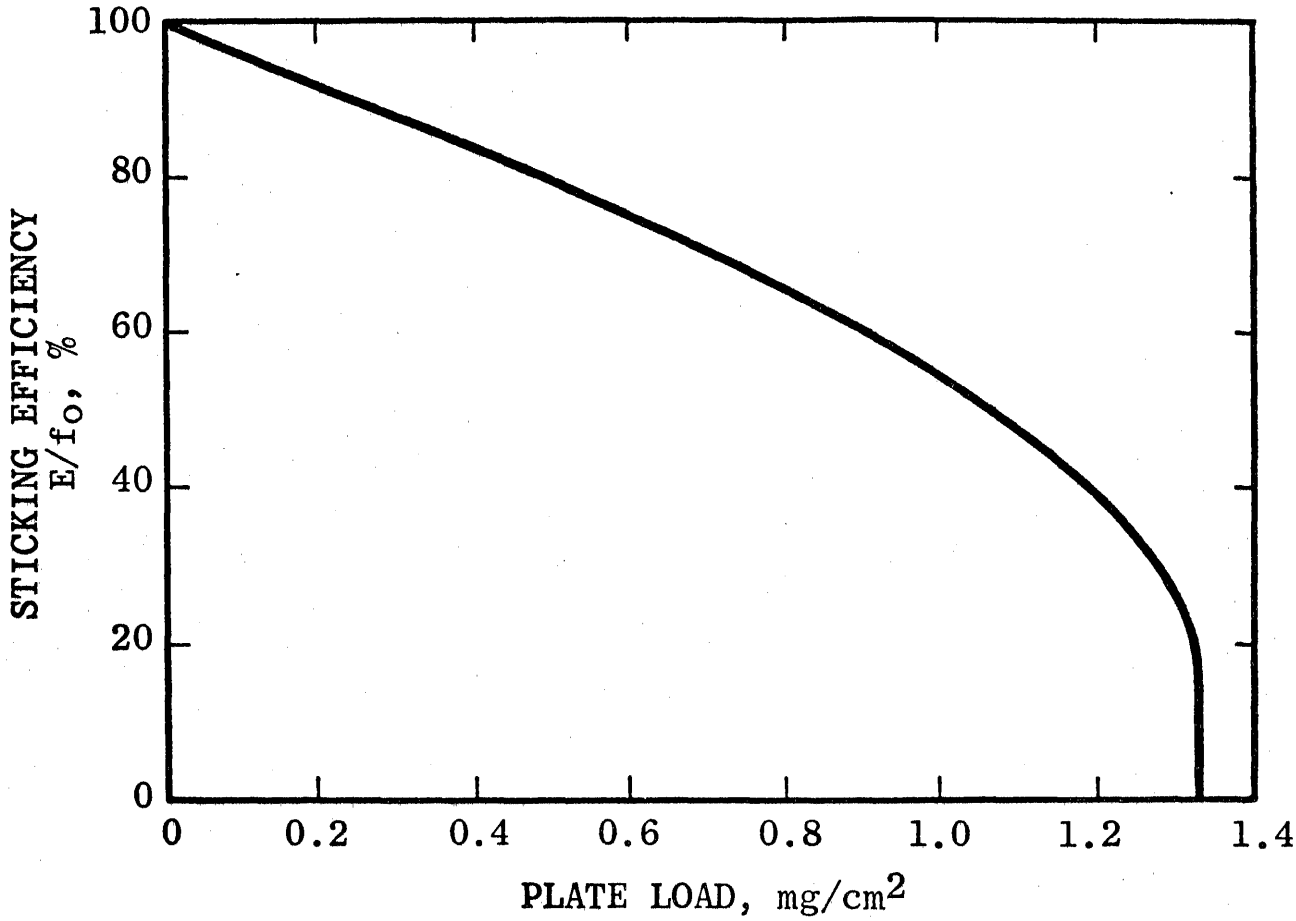

Figure 11

Integrated sticking efficiency vs. plate deposit density calculated for Impactor B from Equation 8. The efficiency goes to zero at 1.33 mg/cm^2 which corresponds to a monolayer of particles on the surface.

It is also necessary to remember that the loading effect is dependent on particle size; the above results were obtained for an aerodynamic diameter of 20 μm. The dependence on particle size can be estimated from the parameter k in Eq. (9) which is inversely proportional to Ad. The area A can be taken to be the orifice area of the various stages of a cascade impactor. Each stage has a 50% cutoff diameter corresponding to a constant value of the Stokes number. In a rectangular slit impactor with constant slit length, the area A is proportional to d and hence $k \alpha d^{-2}$. For a circular slit, $k \alpha d^{\frac{-7}{3}}$. This means that a 2 μm stage will load 100 times faster than the 20 μm stage for the same mass concentration in both size ranges.

Porous Plate Impaction Surface

Discussion of the Concept:

As we have seen, an impaction surface coated with a highly viscous grease remains sticky only for a small loading. Using a less viscous substrate, such as an oil, would allow the particles to become coated with the oil by capillary action to maintain the stickiness of the surface. Unfortunately, such oils are blown off the impaction surface by the air jet. These seemingly contradictory requirements for a liquid surface and a rigid mechanical structure can be met by using a sintered metal plate soaked in a low viscosity oil. Capillary forces maintain a thin liquid surface above the metal structure which provides mechanical support for the bulk of the liquid.

Experimental Tests of the Sintered Plate:

A sintered stainless steel plate (effective filtration pore size quoted at 5 μm) was soaked in a low vapor pressure synthetic machine oil (Teress 030,

Esso Corp., $\eta_{20^\circ C}$ = 0.12 poise) and placed on a glass slide to prevent dripping. The excess oil was allowed to drain off, resulting in a dull appearance to the upper surface of the sintered metal. Slight pressure on the plate would produce visible oil. Under a microscope, small particles could be seen drifting over the metal structure, proving that the upper surfaces were coated with oil. The sintered disc was used as the impaction plate for qualitative experiments with both Impactor A and B. 20 μm potassium biphthalate particles were deposited on the plate for microscopic examination. A well-defined central spot was observed. Most of the particles were submerged in the oil with a few floating on the surface. The metal was still coated with oil.

A long exposure was run with Impactor B, the total load being 60 mg. The result was striking - a "mountain" 0.2 cm high (100 monolayers) and 0.8 cm diameter (the orifice diameter) was formed. Shown in Figure 12, the deposit had a surface which was oil-coated. Thus, capillary action allowed the deposit to grow indefinitely without bounce-off. With the exception of the hot spot and an almost negligible halo near it, no other deposition could be found anywhere on the plate, indicating 100% deposition probability for the impacting particles, independent of the enormous load.

It proved to be impractical to measure the integral deposition efficiency by quantitating the deposit directly because the oil itself turned out to be highly fluorescent. However, the instantaneous efficiency, δE, could be readily measured by the counting technique previously applied to the silicone surface. This was carried out with the results shown in Figure 13 and

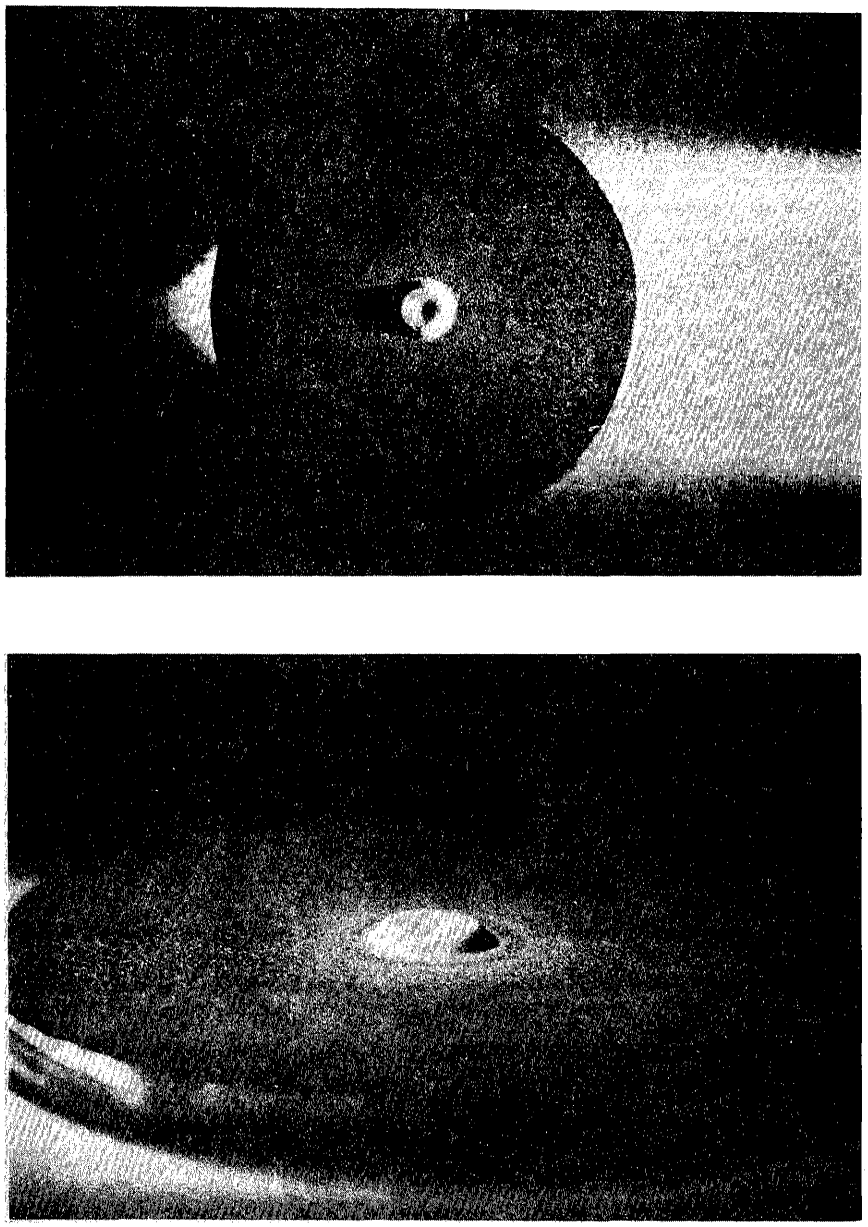

Figure 12. Photographs of the deposit of 60 mg of potassium biphthalate particles on the oil-soaked sintered metal impaction plate using Impactor B.

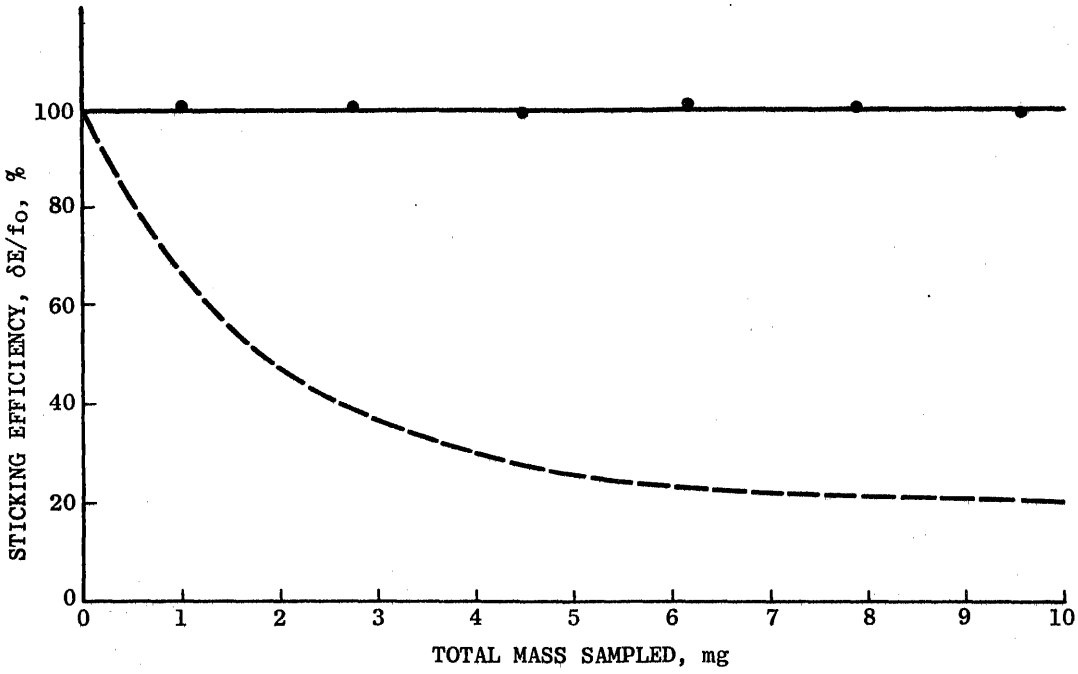

Figure 13

Instantaneous sticking efficiency of the oil-soaked porous plate in Impactor A. The dashed line is the efficiency of the silicone grease-coated plate for comparison.

Figure 14 for Impactor A and B, respectively. Thus, the sticking efficiency was shown to be 100%, independent of load.

Applications of the Porous Plate:

The porous plate has been demonstrated to have essentially 100% efficiency even for enormous loads. One immediate application is for the impaction surface at the inlet of a particle sampler to provide an upper cutoff to particle size. The excellent loading capability could be even further enhanced by operating the surface vertically with a slow flushing of the oil by gravity feed. Another application is for an impactor stage to provide an upper particle size cutoff for an afterfilter, as for example for respirable fraction measurements. It may also be possible to recover and analyze the deposit on the sintered plate itself if suitable techniques are developed.

Summary and Conclusions

The deposition of 20 μm potassium biphthalate particles on a silicone grease-coated impaction surface has been measured as a function of the loading of the surface. A theory was developed which accounts quantitatively for the observations. The results may be used to assess the bounce-off error in cascade impactor measurements.

A new substrate, sintered metal soaked in oil, has been shown to possess an essentially 100% sticking efficiency, independent of the loading.

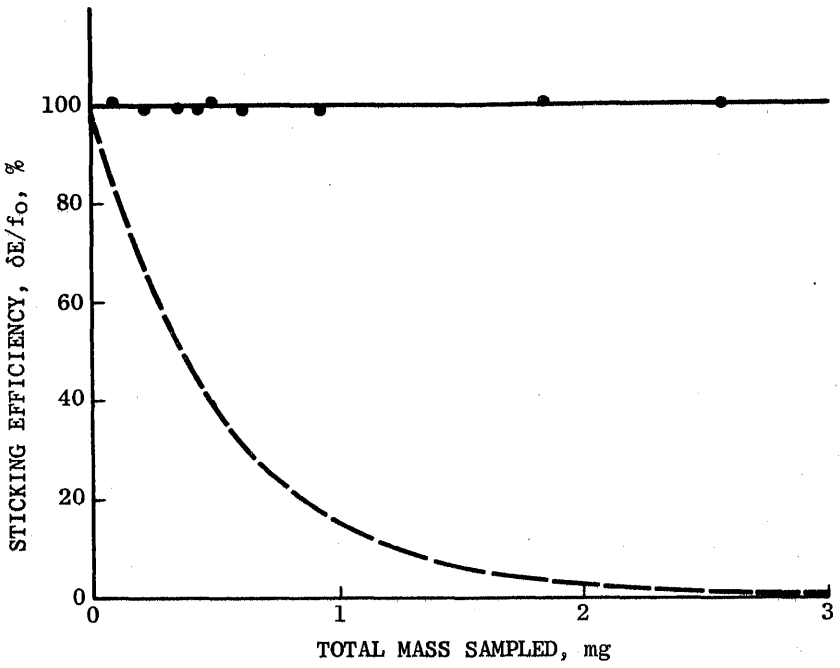

Figure 14

Instantaneous sticking efficiency of the oil-soaked porous plate in Impactor B. The dashed line is the efficiency of the silicone grease-doated plate for comparison.